Journal of Experimental and Theoretical Physics, Vol. 96, No. 2, 2003, pp. 355–382.
Translated from Zhurnal Éksperimental'noĭ i Teoreticheskoĭ Fiziki, Vol. 123, No. 2, 2003, pp. 399–428.

REVIEWS

Density of Prelocalized States in Mesoscopic NS Systems

P. M. Ostrovsky*, M. A. Skvortsov, and M. V. Feigel'man

Landau Institute for Theoretical Physics, Russian Academy of Sciences,
ul. Kosygina 2, Moscow, 117940 Russia
**e-mail: ostrov@itp.ac.ru*

Received September 27, 2002

Abstract—The semiclassical theory of the proximity effect predicts the formation of a gap $E_g \sim \hbar D/L^2$ in the excitation spectrum of a diffusive contact between a normal metal and a superconductor (NS). Mesoscopic fluctuations lead to the emergence of states localized anomalously in the normal metal and weakly linked with the superconducting bank, creating a nonzero density of states for energies lower than E_g. In this review, the behavior of the density of quasiparticle states below a quasi-classical gap is considered for various geometries of the NS system (special attention is paid to SNS junctions) and for the problem of a superconductor with a low concentration of magnetic impurities, in which a similar effect is observed. Analysis is mainly carried out on the basis of a fully microscopic method of the supermatrix σ model; in this method, a nonzero density of states emerges due to instanton configurations with broken supersymmetry. In addition, the results of an alternative approach proceeding from the idea of universality of the spectra of random Hamiltonians with the given symmetry are reviewed. In situations studied using both methods, the results are identical. They include the exact expression for the mean density of states of an NS system in the vicinity of E_g. In the framework of 1D and 2D σ models, the subgap density of states is determined with an exponential accuracy. The contacts with a poor transparency of the NS interface are also considered. It is shown that the number of subgap states in the case of low transparency is much greater than unity. © *2003 MAIK "Nauka/Interperiodica".*

CONTENTS

1. INTRODUCTION

Mesoscopic properties of metals are manifested when the coherence length of conduction electrons is equal to the characteristic size of the sample [1]. These properties are observed most clearly in small samples and are hence accompanied by strong mesoscopic fluctuations.

Superconductivity is another coherent (but not size) effect. It is due to Cooper attraction between electrons. Such an attraction leads to a rearrangement of the ground state of the electron system and radically changes low-energy properties of a metal. In modern experiments, both these conditions can be satisfied simultaneously, which leads to mesoscopic superconductivity. The most interesting and diverse effects are observed for hybrid structures formed by superconducting and normal parts. In the mesoscopic limit, such structures exhibit global coherence leading to phenomena known as the "proximity effect." These phenomena are reduced qualitatively to superconductivity suppression in the superconducting parts and to the emergence of certain superconducting properties in normal regions.

1063-7761/03/9602-0355$24.00

A typical example of such phenomena is the Josephson effect. Cooper pairs tunneling through an insulating layer partly preserve their coherence and, in this way, can carry supercurrent through such a layer. If two superconductors are linked via a normal metal region, an effect of this type has a more complex microscopic structure. In this case, Andreev reflection is a fundamental effect [2].

When an electron is incident on a superconductor–normal metal interface from the side of the normal metal, it cannot penetrate the superconductor since the given energy corresponds to a gap in the spectrum of the superconductor. However, Andreev reflection is possible in this case: the electron is reflected from the normal metal and becomes a hole, while a Cooper pair starts moving in the superconductor. Alternately, this process can be treated as tunneling of a Cooper pair from the superconductor to the normal metal. Although the attraction between electrons vanishes in this case, their combined state is partly coherent. If the normal layer is thin, such a pair may get in the second superconductor, carrying supercurrent in this way. The situation corresponds to a certain electron trajectory connecting two superconducting banks: an electron moving along this trajectory is transformed into a hole upon Andreev reflection, the hole repeating the electron path in the opposite direction, and the trajectory becomes closed after the second Andreev reflection. Such trajectories are allowed when they accommodate an integral number of wavelengths, giving rise to Andreev states [3]. These states form a discrete spectrum and are arranged symmetrically relative to the Fermi level (in the absence of current).

It can be seen from this example that the proximity of the superconductor changes the low-energy spectrum of the normal metal. Similar phenomena, which are also associated with Andreev reflection, may also occur in a simpler case of a single contact between a superconductor and a normal metal. In this case, Andreev states changing the spectrum of the normal metal also appear in the normal region. These changes are determined to a considerable extent by the classical dynamics of electrons in the normal part of the contact. If, for example, the normal region is rectangular in shape and contains no impurities, electron trajectories between two Andreev reflections existing in this region can be infinitely long. This leads to the formation of levels with an arbitrarily low energy and, hence to the absence of a gap in the spectrum. However, the density of states still linearly tends to zero as the Fermi energy is approached [4, 5]. In the general case, this type of spectrum appears when the classical dynamics of electrons in the normal region is integrable.

The opposite limit of chaotic dynamics is realized, for example, in the case of a high density of potential (nonmagnetic) scattering centers (impurities). Under such conditions, the motion of electrons is of the diffusive type. However, a naive attempt to determine the form of the spectrum by analyzing the probability of trajectories of various lengths leads to an erroneous result [6]. Indeed, in the case of random motion, we can always find infinitely long trajectories, but the spectrum will have a gap. The reason for this error lies in the disregard of quantum interference. As a matter of fact, semiclassical diffusive trajectories are broken lines: an electron is scattered successively by a large number of impurities. For two sufficiently long trajectories, we can always find an impurity in common. This means that, in addition to the two corresponding Andreev states, there exist at least two more states: an electron moving along the first trajectory and experiencing scattering by a common impurity passes to the second trajectory, while a hole after Andreev reflection returns to the first trajectory at the same impurity, and vice versa. In view of quantum interference between the above processes, low-lying Andreev levels cannot be described in the naive language of simple trajectories. An appropriate semiclassical technique is well known [7, 8] and is based (in the diffusion case) on the Usadel equation [9]. The result is reduced qualitatively to the emergence of a gap in the density of states on the order of $\hbar/\tau_c$, where τ_c is the characteristic time of diffusion between two Andreev reflections [4, 10–12]. It is determined by the strength and concentration of impurities, the size of the normal region, and the transparency of the interface with the superconductor.

However, the semiclassical theory disregards mesoscopic fluctuations. We can assume, on a qualitative level, that the diffusion coefficient fluctuates, leading to a deviation in the gap width in each specific sample from its mean value. As a result of averaging over possible configurations of impurities, the density of states decreases sharply for a certain energy instead of vanishing, its value being exponentially small for lower energies.

We can formulate the following general statement. If the position of the spectrum edge is determined by a fluctuating physical quantity, averaging over such fluctuations leads to the emergence of a "tail" in the density of states in the forbidden gap. This type of a tail was considered for the first time by Lifshits for an ordinary semiconductor [13]. At present, a large number of fluctuation effects have been observed in various systems (see, for example, [14–16]).

Disordered systems can be treated using a purely phenomenological approach known as the random matrix theory [17–19]. In the framework of this theory, a Hamiltonian is a random matrix and different matrix elements are regarded as uncorrelated (except the relation associated with additional symmetries of the Hamiltonian). In the main order in the large dimension of the matrix, the average density of states of a random Hamiltonian is a "Wigner semicircle,"

$$\langle \rho(E) \rangle = \delta^{-1} \sqrt{1 - E^2/E_0^2},$$

where E_0 is the bandwidth and δ is the mean distance between energy levels at the center of the band.

Owing to its universal nature, the random matrix theory has found wide applications [20] for describing spectral properties of mesoscopic systems. This is manifested in the fact that, in spite of their difference at the level of a microscopic Hamiltonian, the spectra of mesoscopic systems with chaotic dynamics and the spectra of random matrices with identical values of δ are statistically identical. This was demonstrated for the first time by Efetov [21] for a pair correlator of energy levels of a diffusive metallic grain. In this case, both systems are considered at a large distance from the band edge, when the mean density of states can be regarded as independent of energy.

The mean density of states in the Wigner–Dyson ensemble near the band edge vanishes in the semiclassical approximation in proportion to the square root. When corrections are taken into account, an exponentially decreasing tail appears in the semiclassical approximation for energies $|E| > E_0$. In the diffusive NS system, the edge of the spectrum near the gap is also of the root type. If we assume that the shape of the tail is completely determined by the semiclassical behavior of the density of states near the band edge (universality hypothesis), the result of the random matrix theory can be extended to the case of a diffusive NS system. This was done in [22].

Another case when an exponentially small tail appears in the density of states is a superconductor with magnetic impurities. The presence of magnetic impurities suppresses superconductivity. If their concentration is not very high, the gap in the spectrum becomes smaller than in a superconductor without impurities, but does not vanish. However, the impurity concentration may fluctuate in space; consequently the probability of finding an energy level below the mean value of the gap differs from zero. Such a tail in the density of states was calculated in [23, 24] using the method of the nonlinear supermatrix σ model.

Several methods have been developed for calculating electronic properties of systems with disorder. In traditional statistical physics, the properties of a system are mainly determined by the generating functional $Z[J] = \int e^{-S[\Phi, J]} D\Phi$. Various correlation functions, including the density of states, can be expressed in terms of logarithmic derivatives of this functional with respect to sources J. If the system is disordered, all correlation functions should be averaged over the disorder; i.e., the mean value of $\ln Z$ is required. However, the logarithm is a nonlinear function and its averaging is complicated in the general case. One of the methods for overcoming this difficulty, viz., replica trick, was proposed in [25]. In this method, n copies (replicas) are considered instead of a system. The generating functional in this case is Z^n. If the functional can be averaged over disorder for an arbitrary value of n and an analytic continuation in n to point $n = 0$ can be carried out, the formula $\ln Z = \lim_{n \to 0} (Z^n - 1)/n$ can be used.

However, the calculation of the generating functional in the general form for an arbitrary number of the replicas is often a complicated problem. This difficulty is removed in the method of a supermatrix σ model [26]. The essence of this method lies in the addition to physical fields of the same number of Grassmann (anticommuting) fields. For an arbitrary action of the system, the generating functional is equal to unity, and correlation functions are defined by conventional variational derivatives of this functional instead of logarithmic derivatives.

The semiclassical approximation (Usadel equation) corresponds to the evaluation of the generating functional by the steepest descent method. The corresponding saddle point of the action of the nonlinear σ model is supersymmetric; i.e., it has the same form in commuting and Grassmann variables. An exponentially small contribution from low-frequency mesoscopic fluctuations corresponds to other (nonsupersymmetric) saddle points, viz., instantons. Such a calculation was made for the first time in [16] for the density of states at a high Landau level in a 2D system in a magnetic field. The applicability of the steepest descent method in the vicinity of instantons was ensured by the large number of the Landau level. In the case of diffusive NS systems, the corresponding large parameter is the number of conducting channels at the interface between the normal metal and the superconductor.

A generalization of the σ model for diffusive NS systems was proposed in [27] and will be described briefly below. In the same publication, it was pointed out that the subgap density of states corresponds to instantons in this model. The instanton configuration responsible for the emergence of a tail in the density of states in a homogeneous superconductor with magnetic impurities [28] was determined in [23, 24]. Analysis of instantons and calculation of the density of prelocalized states in hybrid systems was carried out in [29]. It was found, among other things, that the contribution to the subgap density of states comes from two instantons. For energies not very close to the threshold, one of these instantons plays the major role, which makes it possible to determine the density of states with an exponential accuracy. In the case when the σ model becomes effectively zero-dimensional (for not very low energies), the preexponential factor was also calculated; the energy dependence of the density of states obtained in this case was found to be the same as in the random matrix theory. The applicability of these results is ensured by a large conductance of the normal region.

We developed this method further in [30]. In particular, we managed to obtain an exact expression for the density of states describing the entire transition region above as well as below the critical energy without using

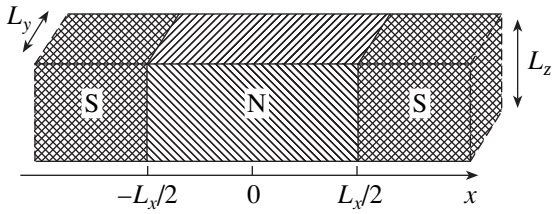

Fig. 1. SNS junction of length L_x. Transverse dimensions are L_y and L_z.

the instanton approximation. In this case also, the form of energy dependence of the density of states is the same as predicted phenomenologically by the random matrix theory. We also considered a long one-dimensional SINIS contact with nonideal interfaces between the normal and superconducting parts. Poor transparency of the interfaces suppresses the proximity effect and reduces the semiclassical gap. When the conductance of an interface becomes smaller than a certain critical value, a transition to another class of universality occurs. The density of states increases as the inverse root function as the energy approaches the threshold from above. In the fluctuation region near the threshold, this divergence is smoothed and transforms into an exponentially decreasing tail described by an expression given in [30]. In contrast to all the cases mentioned above, when the number of states in the region of the fluctuation tail is on average of the order of unity, the number of subgap states in the latter case is parametrically large, and the tail is referred to as strong. In [30], we wrote only the final result for an strong tail due to lack of space. This gap will be made up for in this paper.

This paper is devoted to a review of the results obtained in the framework of the nonlinear supermatrix σ model for mesoscopic superconducting systems. The structure of the review is as follows.

In Section 2, we first consider a semiclassical approach to the evaluation of the density of states. The properties of the semiclassical solution will be required on a later stage for describing possible instantons of the σ model. Then a brief derivation of the σ model for a superconductor is considered. One of the main results of this section is parametrization of the saddle manifold and classification of possible instantons.

The problem of an NS system with absolutely transparent boundaries is solved in Section 3. An exact expression for the density of states near the spectrum edge is derived. The application of the random matrix theory to the problem of an NS contact is considered briefly at the end of the section.

Section 4 generalizes the results to the case of a boundary with an arbitrary transparency. A classification of possible tails of the density of states is constructed depending on the transparency. The case of an strong tail is analyzed separately.

Section 5 is devoted to a system that cannot be described in the framework of the zero-dimensional σ model. These are SNS junctions with a large transverse size, for which the instanton radius is much smaller than the size of the system. A superconductor with magnetic impurities is also considered. At the end of the section, the density of prelocalized states in an SNS junction deep in the gap is calculated with a logarithmic accuracy.

2. GENERAL THEORY

2.1. Semiclassical Approach

Let us first consider a semiclassical method for calculating the density of states in an NS system with transparent boundaries. The Green function of the superconductor provides information on fast oscillations of electrons forming Cooper pairs as well as on a relatively slow motion of a pair as a whole. Averaging the retarded Green function over fast modes in the diffusive case leads to the Usadel equation[1] [9]:

$$\begin{gathered} D\nabla(\hat{g}_R(\mathbf{r})\nabla\hat{g}_R(\mathbf{r})) + i[\tau_z E + i\tau_x\Delta, \hat{g}_R(\mathbf{r})] = 0, \\ \hat{g}_R^2(\mathbf{r}) = 1. \end{gathered} \tag{2.1}$$

Here, $\hat{g}_R(\mathbf{r})$ is a 2×2 matrix in the Nambu space, τ_i are the Pauli matrices acting in the Nambu space, D is the diffusion coefficient, and energy E is measured from the Fermi level. In the angular parametrization $\hat{g}(\mathbf{r}) = \tau_z\cos\theta + \tau_x\sin\theta$, the Usadel equation has the form

$$D\nabla^2\theta + 2iE\sin\theta + 2\Delta\cos\theta = 0. \tag{2.2}$$

We disregard the proximity effect in the superconductor and fix Δ = const in it, while in the region of the normal metal, we assume that Δ is equal to zero. If the size of the normal region exceeds the superconducting coherence length ξ, the gap in the spectrum is on the order of the Thouless energy, which is assumed to be much smaller than Δ; consequently, we can set $\theta = \pi/2$ in the superconductor.

In the normal region of the NS system, the Usadel equation has the form

$$D\nabla^2\theta + 2iE\sin\theta = 0. \tag{2.3}$$

The boundary conditions require that $\theta = \pi/2$ at the interface with the superconductor (ideal interface) and $\nabla_{\mathbf{n}}\theta = 0$ at the free boundary of the normal metal.

The density of states averaged over disorder can be expressed as (ν is the density of states per spin component)

$$\begin{aligned} \langle\rho(E,\mathbf{r})\rangle &= \nu\mathrm{Re}\,\mathrm{tr}(\tau_z\hat{g}(\mathbf{r})) \\ &= 2\nu\mathrm{Re}\cos\theta = 2\nu\mathrm{Im}\sinh\psi, \end{aligned} \tag{2.4}$$

[1] We assume that the phase of the order parameter is equal to zero.

where the substitution $\theta = \pi/2 + i\psi$ has been made, which transforms Eq. (2.3) into the following equation with real coefficients:

$$D\nabla^2\psi + 2E\cosh\psi = 0. \tag{2.5}$$

By way of an example, we consider a one-dimensional SNS junction of length L_x, which is depicted in Fig. 1. In this case, Eq. (2.5) can be integrated easily, which gives the expression for energy in terms of the value of ψ at the middle of the junction:

$$\sqrt{\frac{E}{E_{Th}}} = \int_0^{\psi(0)} \frac{d\psi}{\sqrt{\sinh\psi(0) - \sinh\psi}}, \qquad E_{Th} = \frac{D}{L_x^2}. \tag{2.6}$$

This function is plotted in Fig. 2. It can be seen that the quantity ψ is real (i.e., the density of states is zero) only for energy values smaller than a certain threshold value $E_g = 3.12E_{Th}$. This is exactly the Thouless gap [10, 11].

The example of a 1D junction can be used to establish the following general properties of solutions to the Usadel equation. Equation (2.5) has two real solutions for $E < E_g$. We denote the smaller of these solutions by $\psi_1(\mathbf{r})$ and the larger solution by $\psi_2(\mathbf{r})$. For $E = E_g$, these solutions coincide: $\psi_{1,2}(\mathbf{r}) = \psi_0(\mathbf{r})$. For $E > E_g$, the Usadel equation has two complex solutions, from which we choose the one leading to a positive density of states. From physical considerations, we choose $\psi_1(\mathbf{r})$ under the gap since $\psi_2(\mathbf{r})$ increases indefinitely as the energy tends to zero. It will be shown below, however, that the solution with $\psi_2(\mathbf{r})$ is possible as a fluctuation, which is responsible for a nonzero density of states for energies $E < E_g$.

In the subsequent analysis, we will need a normalized difference of the solutions to the Usadel equation for energy tending to the threshold value (V is the volume of the normal region):

$$f_0(\mathbf{r}) = \lim_{E\to E_g} \frac{\psi_2(\mathbf{r}) - \psi_1(\mathbf{r})}{\sqrt{\int (\psi_2(\mathbf{r}) - \psi_1(\mathbf{r}))^2 \frac{d\mathbf{r}}{V}}}. \tag{2.7}$$

Function $f_0(\mathbf{r})$ satisfies a linear equation which can be derived taking the limit in energy of the difference between the Usadel equations for ψ_1 and ψ_2:

$$D\nabla^2 f_0 + 2E_g f_0 \sinh\psi_0 = 0. \tag{2.8}$$

Expressions for density of states depend on the system geometry only via the following two numerical parameters:

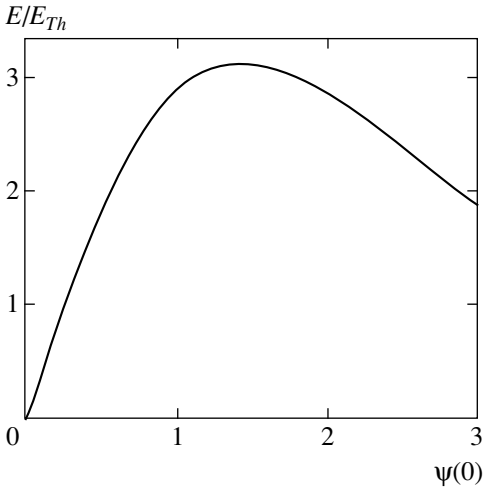

Fig. 2. Dependence of E/E_{Th} on the value of ψ at the middle of a one-dimensional junction (formula (2.6)). The maximum of the function corresponds to the threshold energy value $E_g \approx 3.12E_{Th}$. Below the threshold, the Usadel equation has two solutions, one of which diverges as $E \longrightarrow 0$.

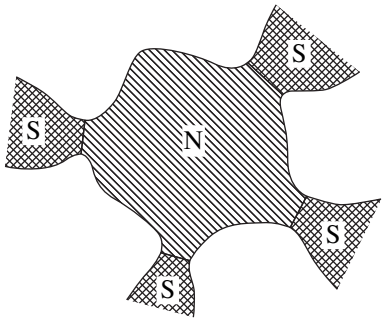

Fig. 3. Contact between a normal grain and superconductors. The main results of Sections 2 and 3 were obtained in the framework of the zero-dimensional σ model for a contact of an arbitrary shape.

$$c_1 = \int \frac{d\mathbf{r}}{V} f_0(\mathbf{r})\cosh\psi_0(\mathbf{r}), \qquad c_2 = \int \frac{d\mathbf{r}}{V} f_0^3(\mathbf{r})\cosh\psi_0(\mathbf{r}). \tag{2.9}$$

In particular, $c_1 \approx 1.15$ and $c_2 \approx 0.88$ for a 1D SNS junction (Fig. 1).

We will consider below a contact of an arbitrary geometry (Fig. 3), assuming that it has only one characteristic scale of length. In this case, the density of states near the threshold can be determined in the approximation of the zero-dimensional σ model (see Subsection 3.2). In the case of a contact whose size along the boundary with superconductors is much larger than their separation, solutions in the form of an

instanton along the larger dimension also exist in addition to the two solutions to the Usadel equation described above. This case requires separate analysis, which will be carried out in Subsection 5.1.

2.2. Derivation of the σ Model

In order to find instanton corrections to the semiclassical density of states, we will briefly describe the derivation of the effective supersymmetric field theory (Efetov σ model [26]) for superconducting systems [27]. The states of an electron in a superconductor are described by the Bogoliubov–De Gennes Hamiltonian, which is a 2×2 matrix in the Nambu space:

$$\mathcal{H} = \tau_z\left(\frac{\mathbf{p}^2}{2m} - \mu + U(\mathbf{r})\right) + \tau_x\Delta(\mathbf{r}). \tag{2.10}$$

We express the density of states in terms of the Green function:

$$\rho(E, \mathbf{r}) = -\frac{1}{\pi}\mathrm{Im}\,\mathrm{tr}\int d\mathbf{r}\,G^R(\mathbf{r}, \mathbf{r}; E). \tag{2.11}$$

The Green function will be calculated using the functional integral[2]

$$G^R(\mathbf{r}, \mathbf{r}'; E) = -i\frac{\int u(\mathbf{r})u^+(\mathbf{r}')e^{-\mathcal{S}[u]}\mathcal{D}u^*\mathcal{D}u}{\int e^{-\mathcal{S}[u]}\mathcal{D}u^*\mathcal{D}u}, \tag{2.12}$$

where the action is defined as

$$\mathcal{S}[u] = -i\int d\mathbf{r}\,u^+(\mathbf{r})(E + i0 - \mathcal{H})u(\mathbf{r}). \tag{2.13}$$

In order to carry out subsequent averaging over disorder, we must get rid of the normalization integral in the denominator of Eq. (2.12). For this purpose, we introduce, in addition to field u, the Grassmann (anticommuting) field χ:

$$\Phi = \begin{pmatrix} \chi \\ u \end{pmatrix}, \tag{2.14}$$

$$G^R(\mathbf{r}, \mathbf{r}'; E) = -i\int u(\mathbf{r})u^+(\mathbf{r}')e^{-\mathcal{S}[\Phi]}\mathcal{D}\Phi^*\mathcal{D}\Phi, \tag{2.15}$$

$$\mathcal{S}[u] = -i\int d\mathbf{r}\Phi^+(\mathbf{r})(E + i0 - \mathcal{H})\Phi(\mathbf{r}). \tag{2.16}$$

Field Φ is formed by four components and belongs to the product of a Nambu space and a supersymmetric Fermi–Bose (FB) space. After averaging over disorder, we must write the effective action for slow modes in $\langle\Phi\Phi^+\rangle$. In addition, we must take into account slow modes in the Cooper channel $\langle\Phi\Phi^T\rangle$ and $\langle\Phi^*\Phi^+\rangle$. For this purpose, we carry out an additional field doubling [26] just now (following notation adopted in [31]):

$$\psi = \frac{1}{\sqrt{2}}\begin{pmatrix} \Phi \\ i\tau_y\Phi^* \end{pmatrix}. \tag{2.17}$$

We will refer to the obtained space as a particle–hole (PH) space. Vector ψ consists of a particle (upper) block and a hole block. We denote by σ_i the Pauli matrix in the PH space and introduce the operation of charge conjugation of supervectors and supermatrices:

$$\bar{\psi} = (C\psi)^T, \quad \bar{A} = CA^TC^T,$$
$$C = -\tau_x\begin{pmatrix} i\sigma_y & 0 \\ 0 & \sigma_x \end{pmatrix}_{FB}. \tag{2.18}$$

Averaging over impurities in Eq. (2.15) leads to an action of the form

$$\mathcal{S}[\psi] = -i\int d\mathbf{r}$$
$$\times\left[\bar{\psi}\left(\Lambda(E + i0) - \frac{\mathbf{p}^2}{2m} + \mu - i\tau_y\Delta(\mathbf{r})\right)\psi + \frac{(\bar{\psi}\psi)^2}{4\pi\nu\tau}\right], \tag{2.19}$$

where we have introduced notation $\Lambda = \sigma_z\tau_z$. The fourth-order term must be decoupled with the help of the Hubbard–Stratonovich transformation. For this purpose, we introduce an 8×8 matrix superfield Q. The transformation leads to the following action:

$$\mathcal{S}[\psi, Q] = -i\int d\mathbf{r}\left[\bar{\psi}\left(\Lambda(E + i0) - \frac{\mathbf{p}^2}{2m} + \mu - i\tau_y\Delta(\mathbf{r}) + \frac{iQ}{2\tau}\right)\psi + \frac{\pi\nu}{8\tau}\mathrm{str}\,Q^2\right]. \tag{2.20}$$

The measure of functional integration over the new field Q is determined from the supersymmetry condition, $\int\exp(-\mathrm{str}\,Q^2)\mathcal{D}Q = 1$.

As a result, the integral over fields ψ becomes a Gaussian integral and can be evaluated. However, there is another difficulty lying in the fact that not all components of ψ and $\bar{\psi}$ are independent. The introduction of the PH space (formula (2.17)) has not resulted in the addition of new variables; old variables have just been regrouped. The action averaged over ψ has the form

$$\mathcal{S}[Q] = \int d\mathbf{r}\,\mathrm{str}\left\{\frac{\pi\nu}{8\tau}Q^2 - \frac{1}{2}\ln\left[\sigma_z(E + i0) - \tau_z\left(\frac{\mathbf{p}^2}{2m} - \mu\right) - \tau_x\Delta + \frac{i\tau_z}{2\tau}Q\right]\right\}. \tag{2.21}$$

This circumstance resulted in the emergence of coefficient 1/2 in front of the logarithm and necessitated the

[2] Symbol $\mathcal{D}u^*\mathcal{D}u$ must be interpreted as follows: $\mathcal{D}u^*\mathcal{D}u = \prod_n\prod_{k=1,2}\pi^{-1}d\mathrm{Re}\,u_n^{(k)}d\mathrm{Im}\,u_n^{(k)}$. Here, $u_n^{(k)}$ are the expansion coefficients of the kth component of vector $u(\mathbf{r})$ in the orthonormal basis of functions.

imposition of the self-conjugate condition on Q:

$$Q = \bar{Q}. \tag{2.22}$$

The obvious saddle point of action (2.21) is $Q = \Lambda$. The approximation of the σ model involves determining a saddle solution which is a slow function of coordinates. To this end, we assume that $Q = e^{-iU/2}\Lambda e^{iU/2}$ and retain in the action the principal terms in gradients Q, in energy E, and in the value of the order parameter Δ. The result of such an expansion is the action of the σ model [27, 29]

$$\mathcal{S}[Q] = \frac{\pi\nu}{8}\int d\mathbf{r} \times \mathrm{str}[D(\nabla Q)^2 + 4iQ(\Lambda(E + i0) + i\tau_x\Delta)], \quad Q^2 = 1, \tag{2.23}$$

and the expression for density of states assumes the form

$$\langle \rho(E, \mathbf{r})\rangle = \frac{\nu}{4}\mathrm{Re}\int \mathrm{str}(k\Lambda Q(\mathbf{r}))e^{-\mathcal{S}[Q]}\mathcal{D}Q. \tag{2.24}$$

Here, we have introduced the following notation for the matrix violating supersymmetry [26]:

$$k = \begin{pmatrix} 1 & 0 \\ 0 & -1 \end{pmatrix}_{FB}. \tag{2.25}$$

2.3. Parametrization of the Q Matrix Manifold

Supermatrix Q has a size of 8×8 and contains 32 complex commuting parameters and the same number of anticommuting (Grassmann) parameters in the general case. Condition $Q = \bar{Q}$ reduces the number of these parameters by half. In accordance with the construction of the σ model, matrix Q has the same structure of eigenvalues as Λ,

$$Q = e^{-iU/2}\Lambda e^{iU/2},$$

which reduces the number of independent parameters to eight complex and eight Grassmann parameters. In this subsection, we construct parametrization of the commuting part of the Q matrix.

The self-conjugate condition for Q leads to anti-self-conjugate for U: $U + \bar{U} = 0$. In addition, we impose the natural condition $\{\Lambda, U\} = 0$, since only such generators can "rotate" matrix Λ. In the absence of Grassmann variables, matrices Q and U split into two independent sectors (FF and BB). Charge conjugation operates in different ways in these two sectors, leading to their different topologies. Matrix U contains the following generators:

$$U^{FF}: \ \sigma_x \quad \sigma_y \quad \sigma_z\tau_x \quad \sigma_z\tau_y$$
$$U^{BB}: \ \sigma_x\tau_z \quad \sigma_y\tau_z \quad \sigma_z\tau_x \quad \sigma_z\tau_y.$$

The FF sector is generated by four pairwise anticommuting generators. Consequently, it forms topologically a 4-dimensional complex sphere S_4. Generators of the BB sector can be divided into two pairs in which they anticommute, while commutativity holds between pairs; i.e., the BB sector is the product of two two-dimensional complex spheres. We choose spherical angles in the form

$$Q^{FF} = \tau_z\cos\theta_F[\sigma_z\cos k_F + \sin k_F(\sigma_x\cos\chi_F + \sigma_y\sin\chi_F)] + \sin\theta_F(\tau_x\cos\varphi_F + \tau_y\sin\varphi_F), \tag{2.26}$$

$$Q^{BB} = [\sigma_z\cos k_B + \tau_z\sin k_B(\sigma_x\cos\chi_B + \sigma_y\sin\chi_B)] \times [\tau_z\cos\theta_B + \sigma_z\sin\theta_B(\tau_x\cos\varphi_B + \tau_y\sin\varphi_B)]. \tag{2.27}$$

An additional symmetry of manifold Q^{BB} is worth noting: the matrix does not change under the simultaneous inversion of both spheres: $(\theta_B, \varphi_B, k_B, \chi_B) \longrightarrow (\pi - \theta_B, \varphi_B + \pi, \pi - k_B, \chi_B + \pi)$. As a result, the BB sector is topologically equivalent to the factorized product $S_2 \times S_2/Z_2$.

The general requirement of the σ model convergence imposes the condition of compactness on the FF sector and noncompactness on the BB sector, which reduces the number of independent variables to four real variables in the FF and BB sectors.

Substituting matrix Q into Eq. (2.23), we obtain the explicit representation of action in terms of the angles introduced above:

$$\mathcal{S} = \frac{\pi\nu}{2}\int d\mathbf{r}(\mathcal{L}^{FF} - \mathcal{L}^{BB}),$$

$$\mathcal{L}^{FF} = D[(\nabla\theta_F)^2 + \sin^2\theta_F(\nabla\varphi_F)^2 + \cos^2\theta_F(\nabla k_F)^2 + \cos^2\theta_F\sin^2 k_F(\nabla\chi_F)^2] + 4iE\cos\theta_F\cos k_F - 4\Delta\sin\theta_F\cos\varphi_F, \tag{2.28}$$

$$\mathcal{L}^{BB} = D[(\nabla\theta_B)^2 + \sin^2\theta_B(\nabla\varphi_B)^2 + (\nabla k_B)^2 + \sin^2 k_B(\nabla\chi_B)^2] + 4iE\cos\theta_B\cos k_B - 4\Delta\sin\theta_B\cos k_B\cos\varphi_B.$$

Angles θ and φ in both sectors have the meaning of the Usadel angle and the phase of the order parameter. In order to determine the saddle configurations of this action for zero phase difference at the contact, we can immediately set $\varphi_F = \varphi_B = 0$. On the saddle solution, angles $\chi_{F,B}$ are independent of coordinates and are completely cyclic: action is independent of $\chi_{F,B}$.

Angle k_F is also equal to zero on a saddle solution. In the BB sector, it is convenient to carry out the substitution of variables:

$$\theta_B = \frac{\alpha+\beta}{2}, \quad k_B = \frac{\alpha-\beta}{2}. \tag{2.29}$$

In terms of angles θ_F, α, and β, action has the simple form

$$\mathcal{S}[\theta_F, \alpha, \beta] = 2S_0[\theta_F] - S_0[\alpha] - S_0[\beta], \tag{2.30}$$

$$S_0[\theta] = \frac{\pi\nu}{4}\int d\mathbf{r} \times [D(\nabla\theta)^2 + 4iE\cos\theta - 4\Delta\sin\theta]. \tag{2.31}$$

2.4. Saddle Points

Variation of action (2.31) leads to Eq. (2.2). Thus, a saddle point can be described by the Usadel equation in each of the three variables (θ_F, α, and β). In accordance with Subsection 2.1, the Usadel equation has two solutions: $\theta_1(\mathbf{r})$ and $\theta_2(\mathbf{r})$. (The only exception is the situation when the contact size along the interface with superconductors is much larger than their separation; this case will be treated separately in Subsection 5.1.) Since solutions $\theta_1(\mathbf{r})$ and $\theta_2(\mathbf{r})$ coincide for $E = E_g$, the mode transforming $\theta_1(\mathbf{r})$ into $\theta_2(\mathbf{r})$ becomes softer near the threshold. As a result, the functional integral over $Q(\mathbf{r})$ becomes an ordinary integral over supermatrix Q; i.e., a transition to the zero-dimensional σ model occurs.

Thus, in the zero-dimensional case, there exist $2^3 = 8$ saddle solutions in all. If we choose solution θ_1 in all three variables θ_F, α, and β, we automatically obtain $\theta_B = \theta_1$, $\theta_F = \theta_1$, and $k_B = 0$; i.e., the FF and BB sectors are identical. Expanding action (2.28) up to the second order in fluctuations in the vicinity of such a saddle point, we find that the superdeterminant of this quadratic form is equal to unity, which is a direct consequence of the FF–BB symmetry of the solution. The functional integral (2.24) in this case is reduced to (2.4). Thus, the semiclassical approximation can be obtained from the σ model in the steepest descent approximation in the vicinity of a supersymmetric saddle point.

Higher orders of the expansion of action near a supersymmetric saddle point correspond to perturbation corrections to a semiclassical result. These corrections were analyzed in [27], where it was shown that their inclusion leads to renormalization of E_g. In this case, the density of states below the renormalized value of the gap vanishes as before. The average density of states is found to be finite in the entire energy range only if we take into account other saddle points (instantons). In other words, we must use the second solution of the Usadel equation in one or several variables θ_F, α, and β.

The density of states vanishes when $\mathrm{Re}\,\theta_{1,2} = \pi/2$. This equality is valid for both Usadel solutions for $E < E_g$. How is it that an instanton may contribute to the subgap density of states? As a matter of fact, a quadratic action in the vicinity of an instanton saddle point contains a negative eigenvalue; consequently, an imaginary unity appears in the integral over fluctuations in the vicinity of the instanton and, as a result, a nonzero density of states appears below the gap.

Let us consider instantons, which can appear in the zero-dimensional case. First, we note the obvious inequality

$$S_0[\theta_1] > S_0[\theta_2]. \tag{2.32}$$

In order to obtain a positive action (2.30) at an instanton, we must fix $\theta_F = \theta_1$. It will be shown below (see Subsection 3.2) that the saddle point $\theta_F = \theta_2$ cannot be attained by deforming the integration contour in the variables of the FF sector under the condition of convergence of the σ model. Thus, we are left with three nonstandard saddle solutions in the BB sector: $(\alpha, \beta) = (\theta_2, \theta_1)$, $(\alpha, \beta) = (\theta_1, \theta_2)$, and $(\alpha, \beta) = (\theta_2, \theta_2)$. At first glance, the two first solutions break the symmetry in angle χ_B. In actual practice, this symmetry is restored due to the fact that there exists a full saddle ring containing both these points. Different points of this ring differ in angle χ_B. In particular, points $(\alpha, \beta) = (\theta_2, \theta_1)$ and $(\alpha, \beta) = (\theta_1, \theta_2)$ can be obtained from each other by changing angle χ_B by π. This ring will be referred to as the first instanton. The third solution, $(\alpha, \beta) = (\theta_2, \theta_2)$, is an isolated saddle point that will be referred to as the second instanton.

Both instanton solutions can be presented in the form

$$Q_0 = e^{-iU_0/2}\Lambda e^{iU_0/2} = \Lambda e^{iU_0}, \tag{2.33}$$

where

$$U_0^{FF} = \sigma_z\tau_y\theta_F,$$
$$U_0^{BB} = \sigma_z\tau_y\theta_B + \tau_z k_B(\sigma_y\cos\chi_B - \sigma_x\sin\chi_B). \tag{2.34}$$

On the ring of the first instanton, we have

$$\theta_F = \frac{\pi}{2} + i\psi_1(\mathbf{r}), \quad \theta_B = \frac{\pi}{2} + i\frac{\psi_1(\mathbf{r}) + \psi_2(\mathbf{r})}{2},$$
$$k_B = i\frac{\psi_2(\mathbf{r}) - \psi_1(\mathbf{r})}{2}, \quad \chi_B \in [0, 2\pi), \tag{2.35}$$

while on the second instanton we have

$$\theta_F = \frac{\pi}{2} + i\psi_1(\mathbf{r}), \quad \theta_B = \frac{\pi}{2} + i\psi_2(\mathbf{r}),$$
$$k_B = 0. \tag{2.36}$$

The instanton action can be easily determined in the vicinity of the semiclassical edge E_g of the spectrum. We make use of the fact that the two solutions of the

Usadel equation coincide at the threshold: $\theta_{1,2}(\mathbf{r}) = \theta_0(\mathbf{r}) = \pi/2 + i\psi_0(\mathbf{r})$. For $E \longrightarrow E_g$, their difference is proportional to function $f_0(\mathbf{r})$ defined by formula (2.7).

In order to evaluate the action at an instanton, we substitute $\theta(\mathbf{r}) = \pi/2 + i\psi_0(\mathbf{r}) + igf_0(\mathbf{r})$ into expression (2.31) and expand it in g and dimensionless energy ε measured from the threshold,

$$\varepsilon = \frac{E_g - E}{E_g}. \tag{2.37}$$

This gives

$$\begin{aligned} S_0[\theta] &= S_0[\theta_0] \\ &+ \frac{\pi\nu}{4}\int d\mathbf{r}\Big[2gf_0(D\nabla^2\psi_0 + 2E_g\cosh\psi_0) \\ &+ g^2 f_0(D\nabla^2 f_0 + 2E_g f_0\sinh\psi_0) \\ &- 4E_g\varepsilon g f_0\cosh\psi_0 + \frac{2}{3}E_g g^3 f_0^3\cosh\psi_0\Big]. \end{aligned} \tag{2.38}$$

The first term in the integrand vanishes in accordance with the Usadel equation, and the second vanishes in accordance with Eq. (2.8). Thus, we can represent S_0 in the form of a cubic polynomial in g:

$$S_0[\theta] = \text{const} + \frac{\pi E_g}{2\delta}\Big[-2c_1\varepsilon g + \frac{c_2}{3}g^3\Big]. \tag{2.39}$$

Here, we have introduced the mean level spacing $\delta = (\nu V)^{-1}$. The expression obtained has two extrema,

$$g_\pm = \pm\sqrt{\tilde{\varepsilon}}, \quad \tilde{\varepsilon} = \frac{2c_1}{c_2}\varepsilon, \tag{2.40}$$

corresponding to two solutions to the Usadel equation (g_+ corresponds to solution $\theta_2(\mathbf{r})$ and g_- to solution $\theta_1(\mathbf{r})$). Substituting these solutions into Eq. (2.30), we obtain the following expression for the action of the first instanton:

$$\mathcal{S}_1 = S_0[\theta_1] - S_0[\theta_2] = \frac{4}{3}\tilde{G}\tilde{\varepsilon}^{3/2}; \tag{2.41}$$

here, we have introduced the notation

$$\tilde{G} = \frac{\pi c_2 E_g}{2\delta}. \tag{2.42}$$

For a planar junction (see Fig. 1), this quantity is of the order of the dimensionless conductance of the normal region: $\tilde{G} \approx 0.34G_N$, where $G_N = 4\pi\nu DL_yL_z/L_x$.

In accordance with Eq. (2.30), action $\mathcal{S}_2$ of the second instanton is twice as large as action $\mathcal{S}_1$ of the first instanton. Consequently, their relative contribution to the density of states is determined by the value of $\mathcal{S}_1$. For $\mathcal{S}_1 \gg 1$, the contribution of the second instanton is exponentially suppressed as compared to the contribution of the first instanton, which is also exponentially small. This regime, which corresponds to energies differing considerably from the threshold value, will be considered in Subsection 3.1. In the case of exact equality $E = E_g$, action $\mathcal{S}_1$ vanishes. For this reason, there exists a fluctuating region in the vicinity of the threshold, which is determined by inequality $|\varepsilon| \lesssim \tilde{G}^{-2/3}$, where $\mathcal{S}_1 \lesssim 1$, so that the contributions from both instantons are of the same order of magnitude and, hence, cannot be separated.

The exact solution taking into account both instantons in the entire energy range will be given in Subsection 3.2.

2.5. Parametrization of Fluctuations

In order to apply the steepest descent method with the saddle point determined by us, we must evaluate the integral over all possible fluctuations of the Q matrix in the vicinity of the instanton. For this purpose, we expand the action in the matrix form up to the second order in the vicinity of the saddle and then propose a parametrization diagonalizing the quadratic form of the action.

We introduce matrix W describing fluctuations:

$$\begin{aligned} &Q = e^{-iU_0/2}e^{-iW/2}\Lambda e^{iW/2}e^{iU_0/2}, \\ &\{\Lambda, W\} = 0, \quad W + \overline{W} = 0. \end{aligned} \tag{2.43}$$

We must now substitute matrix Q expressed in terms of W into action (2.23) and expand it up to the second order in W. We assume that $\Delta = 0$ since we are going to operate with this action only in the normal region. The quadratic form of the action can be written as

$$\begin{aligned} \mathcal{S}^{(2)}[W] &= \frac{\pi\nu}{8}\int d\mathbf{r} \\ &\times \text{str}\Big[D(\nabla W)^2 + \frac{D}{4}[\nabla U_0, W]^2 - 2iE\Lambda Q_0 W^2\Big]. \end{aligned} \tag{2.44}$$

Matrix W, as well as Q, contains eight commuting parameters and the same number of Grassmann parameters. The complete parametrization of this matrix, in which action (2.44) is diagonal, is given in Appendix A. Quadruples a, b, c, d and m, n, p, q of real variables parametrize the FF and BB sectors of matrix W, respectively, while eight Grassmann variables (λ, μ, ζ, κ, η, γ, ξ, ω) parametrize the anticommuting component of

matrix W. The quadratic part of the action in terms of new variables assumes the form

$$\begin{aligned}\mathcal{S}^{(2)} &= (a\hat{\mathbb{O}}^{+}_{\theta_F\theta_F}a) + (b\hat{\mathbb{O}}^{-}_{\theta_F\theta_F}b) + (c\hat{\mathbb{O}}^{+}_{\theta_F\theta_F}c)\\ &+ (d\hat{\mathbb{O}}^{+}_{\theta_F\theta_F}d) + (m\hat{\mathbb{O}}^{+}_{\alpha\beta}m) + (n\hat{\mathbb{O}}^{-}_{\alpha\beta}n)\\ &+ (p\hat{\mathbb{O}}^{-}_{\beta\beta}p) + (q\hat{\mathbb{O}}^{-}_{\alpha\alpha}q) + (\lambda\hat{\mathbb{O}}^{+}_{\alpha\theta_F}\eta)\\ &+ (\mu\hat{\mathbb{O}}^{+}_{\beta\theta_F}\gamma) + (\kappa\hat{\mathbb{O}}^{-}_{\beta\theta_F}\omega) + (\zeta\hat{\mathbb{O}}^{-}_{\alpha\theta_F}\xi).\end{aligned} \tag{2.45}$$

Here, we have introduced operators $\hat{\mathbb{O}}^{\pm}_{\alpha\beta}$ acting in accordance with the rule

$$\begin{aligned}(a\hat{\mathbb{O}}^{\pm}_{\alpha\beta}b) &= \frac{\pi\nu}{8}\int d\mathbf{r}\,a(\mathbf{r})\\ &\times\left[-D\nabla^2 - \frac{D}{4}(\nabla\alpha \pm \nabla\beta)^2 - iE(\cos\alpha + \cos\beta)\right]b(\mathbf{r}).\end{aligned} \tag{2.46}$$

Operators $\hat{\mathbb{O}}$ possess a discrete spectrum since fluctuations occur in a bounded space of the normal region. We denote the eigenvalues of operator $\hat{\mathbb{O}}^{\pm}_{\alpha\beta}$ by $(\mathscr{E}^{\pm}_{\alpha\beta})_n/\delta$, where n runs through values from 0 to ∞. It follows from Eq. (2.46) that the difference between the first excited state and the ground state of any operator $\hat{\mathbb{O}}$ is on the order of $(\mathscr{E}^{\pm}_{\alpha\beta})_1 - (\mathscr{E}^{\pm}_{\alpha\beta})_0 \approx E_g$. The ground state energy of operators $\hat{\mathbb{O}}^{+}$ has the scale of E_g. The ground state of operator $\hat{\mathbb{O}}^{-}_{\theta_1\theta_2}$ has zero energy, and its eigenfunction is equal to $\sin((\theta_1 - \theta_2)/2)$ to within normalization. Exactly at the threshold, for $E = E_g$, the ground state energies of operators $\hat{\mathbb{O}}^{-}_{\theta_1\theta_1}$ and $\hat{\mathbb{O}}^{-}_{\theta_2\theta_2}$ are also equal to zero. As we move away from the threshold towards lower energies, $(\mathscr{E}^{-}_{\theta_1\theta_1})_0$ becomes positive and $(\mathscr{E}^{-}_{\theta_2\theta_2})_0$ becomes negative. In the limit $E_g - E \ll E_g$, the inequality $\left|(\mathscr{E}^{-}_{\alpha\beta})_0\right| \ll E_g$ holds.

The spectrum of operators $\hat{\mathbb{O}}$ determines the masses $\mathscr{E}_n$ of various fluctuations in the vicinity of instanton saddle solutions. Depending on the value of these masses, we can single out the following three types of fluctuations.

(i) Zero modes. Strictly zero modes include Grassmann Goldstone modes restoring the supersymmetry broken by a saddle solution (mode $\zeta\xi$ for the first instanton and modes $\zeta\xi$ and $\kappa\omega$ for the second instanton) as well as the Goldstone mode n restoring the symmetry of the first instanton in angle χ_B. Zero modes correspond to the ground state of operator $\hat{\mathbb{O}}^{-}_{\theta_1\theta_2}$.

(ii) Soft modes. These include fluctuations of variables b, p, and q as well as mode $\kappa\omega$ (in the case of the first instanton), which correspond to the ground states of operators $\hat{\mathbb{O}}^{-}_{\theta_1\theta_1}$ and $\hat{\mathbb{O}}^{-}_{\theta_2\theta_2}$. If $E \longrightarrow E_g$, the mass of soft modes tends to zero.

(iii) Hard modes. These modes have a mass on the order of the Thouless energy and above, so that their fluctuations are small in parameter $E_g/\delta \sim G_N \gg 1$. This inequality ensures the validity of the steepest descent method. Hard modes include all eigenstates of operators $\hat{\mathbb{O}}^{+}$ and excited states of operators $\hat{\mathbb{O}}^{-}$.

3. CONTACT WITH IDEAL INTERFACES

We will consider a contact with ideal interfaces between a superconductor and a normal metal. Let us first consider a contact for energies close to the threshold energy, but still differing from it, $\tilde{G}^{-2/3} \ll (E_g - E)/E_g \ll 1$, for which the approximation of the zero-dimensional σ model is applicable. In this energy range, the main contribution to the density of states comes from the first instanton. The main exponent in the expression for density of states is defined by formula (2.41). We will now calculate the preexponential factor and then construct a more complete theory, taking into account the contributions from the second instanton. As a result, we will obtain an exact (naturally, in the steepest descent approximation in hard modes, which is controlled by parameter $\tilde{G} \gg 1$) expression describing the average density of states both below and above the threshold energy, including the entire fluctuation region. The form of the obtained expression coincides with the predictions of the random matrix theory for the edge of the spectrum, which may serve as a microscopic substantiation of the hypothesis put forth in [22].

3.1. Single-Instanton Solution

In this subsection, we determine the contribution of the first instanton to the average density of states. We consider a region in the vicinity of the semiclassical edge E_g of the spectrum, but outside the fluctuation region: $\tilde{G}^{-2/3} \ll \varepsilon \ll 1$, in which we can disregard the contribution from the second instanton. According to the classification given in Subsection 2.4, action (2.45) at the first instanton $(\theta_F, \alpha, \beta) = (\theta_1, \theta_2, \theta_1)$ has a zero mode in variable n, a Grassmann zero mode $\zeta\xi$, and soft modes in variables b, p, q, and $\kappa\omega$. All the remaining modes are hard.

Inequality $\tilde{G} \gg 1$ guarantees that, while integrating over hard fluctuations, we can disregard the preexponential factor in formula (2.24). In this case, integration

becomes trivial and gives the superdeterminant of the quadratic form (2.45):

$$\sqrt{\frac{\det\hat{\mathbb{O}}^{+}_{\theta_1\theta_2}\det'\hat{\mathbb{O}}^{-}_{\theta_1\theta_2}}{\det\hat{\mathbb{O}}^{+}_{\theta_1\theta_1}\det'\hat{\mathbb{O}}^{-}_{\theta_1\theta_1}}} = 1 + O(\varepsilon). \tag{3.1}$$

Here, the prime denotes elimination of the lowest eigenvalue, and the equality follows from the estimate $(\mathscr{E}^{\pm}_{\theta_1\theta_2})_n - (\mathscr{E}^{\pm}_{\theta_1\theta_1})_n = O(\varepsilon)$ (inequality $n > 0$ holds for eigenvalues $\mathscr{E}^{-}$) and from the asymptotic form $(\mathscr{E}^{\pm}_{\alpha\beta})_n \propto n^2E_g$, which is valid for $n \gg 1$. Thus, hard fluctuations make zero contribution to the density of states in the limit in question.

It remains for us to consider soft and zero modes. It should be noted that zero modes in variables n and $\zeta\xi$ behave differently upon a deviation from the instanton solution. The zero mode in variable n corresponds to rotation through angle χ_B and remains massless for any (not necessarily saddle) noncoinciding values of α and β. On the other hand, the Grassmann zero mode $\zeta\xi$ acquires a mass upon a deviation from the instanton solution. Such a behavior is determined by the necessity of satisfying condition $\int e^{-S[Q]}DQ = 1$, which would be impossible if the Grassmann mode remained a strictly Goldstone mode upon deviation from the saddle solution.

Thus, in variables ζ and ξ, it is insufficient to confine analysis to the quadratic action (2.45); it is necessary to continue the expansion to the next order in fluctuations. We can prove[3] that, in the third order, ζ and ξ are entangled only with variable q. With respect to the remaining soft modes b, p, and $\kappa\omega$, we can take a Gauss integral, making use of the fact that our analysis is carried out outside the fluctuation region. The contribution from commuting variables in the emerging superdeterminant exactly cancels the contribution from Grassmann variables.

As a result, we are left with the integral with respect to variables n, $\zeta\xi$, and q. The eigenfunction of the corresponding operators $\hat{\mathbb{O}}^{-}$ near the threshold is $f_0(\mathbf{r})$; consequently, we can single out the coordinate dependence: $n = \tilde{n}f_0(\mathbf{r})$, etc. We must retain in the action the term $\tilde{q}^2(\mathscr{E}^{-}_{\theta_2\theta_2})_0/\delta$ originating from Eq. (2.45) as well as the term proportional to $\tilde{\zeta}\tilde{\xi}\tilde{q}$ and removing degeneracy of the Grassmann zero mode.

In order to calculate the minimal eigenvalue of operator $\hat{\mathbb{O}}^{-}_{\theta_2\theta_2}$ in the main order in deviation from the threshold, we can use function f_0, since it is an eigenfunction of operators $\hat{\mathbb{O}}^{-}$ for $E = E_g$, which corresponds to a zero eigenvalue. Substituting $\theta_2 = \pi/2 + i\psi_0 + i\sqrt{\tilde{\varepsilon}}f_0$ into formula (2.46) and expanding in $\sqrt{\tilde{\varepsilon}}$, we obtain

$$\frac{(\mathscr{E}^{-}_{\theta_2\theta_2})_0}{\delta} = \frac{\pi\nu}{8}\int d\mathbf{r} \times f_0[-D\nabla^2 - 2E_g\sinh(\psi_0 + \sqrt{\tilde{\varepsilon}}f_0)]f_0 = -\frac{\tilde{G}}{2}\sqrt{\tilde{\varepsilon}}. \tag{3.2}$$

In order to calculate the term proportional to $\tilde{\zeta}\tilde{\xi}\tilde{q}$ in the action, it is sufficient to use expression (2.45), which gives $\tilde{\zeta}\tilde{\xi}(\mathscr{E}^{-}_{\theta_1\alpha})_0/\delta$; while calculating this term, we must take into account the difference between angle α and the instanton solution θ_2 associated with fluctuation of q. Using formula (A.4), we assume that $\alpha = \theta_2 - i\tilde{q}/\sqrt{2}f_0$. Expanding in $\tilde{q}$ analogously to relation (3.2), we obtain

$$\frac{(\mathscr{E}^{-}_{\theta_1\alpha})_0}{\delta} = \frac{\tilde{G}\tilde{q}}{4\sqrt{2}}. \tag{3.3}$$

Let us now calculate the preexponential factor in Eq. (2.24). For the density of states averaged over the volume, we must evaluate the integral

$$\begin{aligned}\frac{\nu}{4}\int d\mathbf{r}\,\mathrm{str}(k\Lambda Q) &= \frac{\nu}{2}\int d\mathbf{r}[2\cos\theta_F + \cos\alpha + \cos\beta] \\ &= -\frac{i\nu}{2}\int d\mathbf{r}[3\sinh(\psi_0 - \sqrt{\tilde{\varepsilon}}f_0) \\ &+ \sinh(\psi_0 + (\sqrt{\tilde{\varepsilon}} - \tilde{q}/\sqrt{2})f_0)] = \mathrm{const} + \frac{ic_1\tilde{q}}{2\sqrt{2}\delta}.\end{aligned} \tag{3.4}$$

Here, we have singled out the imaginary constant that makes zero contribution to the density of states.[4] While evaluating the preexponential factor (3.4), we have omitted the Grassmann variables ζ and ξ, which are thus retained only in the action. It can be proved that the contribution from the omitted terms is small in parameter $\sqrt{\tilde{\varepsilon}}$.

[3] In fact, eigenvalue $(\mathscr{E}^{-}_{\alpha\theta_F})_0$ is a function of both q and b (see formula (A.4)). If, however, we take into account the term on the order of $b\zeta\xi$ in the action, this will lead to the emergence of term $\tilde{b}\tilde{q}$ in the preexponential factor of formula (3.5), which is not an imaginary quantity as required and makes zero contribution to the density of states.

[4] The coefficient of $\tilde{q}$ is also imaginary; however, the subsequent integration with respect to $\tilde{q}$ (see relation (3.5)) will be carried out along the imaginary axis; consequently, the density of states will be due to the retained term.

Taking into account relations (3.2)–(3.4), we obtain the following expression for the density of states:

$$\langle\rho\rangle = e^{-\mathcal{S}_0}\mathrm{Re}\int\frac{d\tilde{n}d\tilde{q}}{\pi}d\tilde{\zeta}d\tilde{\xi}\frac{ic_1\tilde{q}}{2^{3/2}\delta} \times\exp\left[-\frac{\tilde{G}}{2}\left(-\sqrt{\tilde{\varepsilon}}\tilde{q}^2+\frac{\tilde{q}\tilde{\zeta}\tilde{\xi}}{2\sqrt{2}}\right)\right] = -\frac{c_1\tilde{G}}{16\pi\delta}e^{-\mathcal{S}_0}\mathrm{Im}\int d\tilde{n}d\tilde{q}\tilde{q}^2\exp\left(\frac{\tilde{G}}{2}\sqrt{\tilde{\varepsilon}}\tilde{q}^2\right). \quad (3.5)$$

In order to integrate with respect to the zero mode $\tilde{n}$, we use relation (A.4):

$$n = 2i\sin k_B\chi_B = (\psi_1-\psi_2)\chi_B = -2\sqrt{\tilde{\varepsilon}}f_0\chi_B,\quad \tilde{n} = -2\sqrt{\tilde{\varepsilon}}\chi_B,\quad \int d\tilde{n} = 4\pi\sqrt{\tilde{\varepsilon}}. \quad (3.6)$$

For the convergence of the integral with respect to $\tilde{q}$, we must choose the integration contour along the imaginary axis, which gives us the required imaginary unity. Substituting the instanton action (2.41), we finally obtain the density of states in the form

$$\langle\rho\rangle = \frac{c_1}{\delta}\sqrt{\frac{\pi}{8\tilde{G}\sqrt{\tilde{\varepsilon}}}}\exp\left(-\frac{4}{3}\tilde{G}\tilde{\varepsilon}^{3/2}\right), \quad (3.7)$$

where quantities $\tilde{\varepsilon}$ and $\tilde{G}$ are defined by formulas (2.37), (2.40), and (2.42). Formula (3.5) describes the behavior of the average density of states outside the fluctuation regions for $\tilde{G}^{-2/3} \ll \varepsilon \ll 1$.

We will also determine the density of states above the threshold. In this region, we have $\sqrt{\tilde{\varepsilon}} = i\sqrt{|\tilde{\varepsilon}|}$. We do not need the instanton solution since the main contribution to integral (2.24) comes from the neighborhood of the supersymmetric saddle point $\theta_F = \alpha = \beta = \theta_1 = \pi/2 + i\psi_0 - \sqrt{|\tilde{\varepsilon}|}f_0$. The integral over fluctuations becomes equal to unity, and the preexponential factor has the form

$$\langle\rho\rangle = \frac{\nu}{4}\mathrm{Re}\int d\mathbf{r}\,\mathrm{str}(k\Lambda Q) = 2\nu\mathrm{Im}\int d\mathbf{r}\sinh(\psi_0+i\sqrt{|\tilde{\varepsilon}|}f_0) = \frac{2c_1}{\delta}\sqrt{|\tilde{\varepsilon}|}. \quad (3.8)$$

Two results for the density of states above and below the threshold energy are "sewn together": the values on the left and right of the fluctuation region turn out to be of the same order of magnitude:

$$\langle\rho\rangle|_{\varepsilon\sim\pm\tilde{G}^{-2/3}} \sim \frac{1}{\tilde{G}^{1/3}\delta}. \quad (3.9)$$

Another characteristic property of the subgap density of states (3.7) is that the total number of energy levels under the gap is independent of $\tilde{G}$ and is of the order of unity:

$$\mathcal{N} \sim \int_0^{E_g}\langle\rho(E)\rangle dE \sim \frac{E_g}{\tilde{G}\delta} \sim 1. \quad (3.10)$$

It will be shown in Section 4 that this property may be violated for a contact with tunnel boundaries in the limit of a so-called strong tail.

3.2. Exact Solution near the Threshold

Let us now calculate the density of states taking into account the second instanton. The result obtained will be exact in the entire fluctuation region in the vicinity of the critical energy.

It was proved above that hard modes make zero contribution to the density of states. For this reason, in the general case, we are left with eight quasi-zero modes corresponding to the minimal eigenvalues of operators $\hat{\mathbb{O}}^-$: $b, n, p, q, \zeta\xi$, and $\kappa\omega$ (as we seek an exact solution, the division into zero and soft modes, which was made for saddle solutions, becomes meaningless). We take into account the coordinate dependence using the representation $n = \tilde{n}f_0(\mathbf{r})$, etc., and introduce, instead of variables $\tilde{b}$, $\tilde{p}$, and $\tilde{q}$, symmetric variables interpolating between the two solutions to the Usadel equation:

$$\alpha = \frac{\pi}{2}+i\psi_0+iuf_0,\quad \beta = \frac{\pi}{2}+i\psi_0+iVf_0,\quad \theta_F = \frac{\pi}{2}+i\psi_0+iwf_0. \quad (3.11)$$

We must now expand the action up to cubic terms in quasi-zero variables. Calculations similar to those used while deriving Eqs. (2.39), (3.2), and (3.3) lead to the following expression for action:

$$\mathcal{S} = \tilde{G}\left[\tilde{\varepsilon}(u+V-2w)-\frac{u^3+V^3-2w^3}{3} -\tilde{\zeta}\tilde{\xi}\frac{u+w}{4}-\tilde{\kappa}\tilde{\omega}\frac{V+w}{4}\right]. \quad (3.12)$$

Eight extrema of this action (two for each of variables u, V, and w) correspond to a supersymmetric saddle and to different instantons. Analogously to relation (3.4), we obtain the following expression for the preexponential factor:

$$\frac{\nu}{4}\int d\mathbf{r}\,\mathrm{str}(k\Lambda Q) = -\frac{ic_1}{2\delta}(u+V+2w). \quad (3.13)$$

We must now establish a correct measure of integration. The relation between variables u, V, w and $\tilde{p}$, $\tilde{q}$, $\tilde{b}$ follows from relations (A.4). Since the measure of

integration with respect to $\tilde{p}$, $\tilde{q}$, $\tilde{b}$ is trivial (see relation (A.5)), we conclude that

$$\mathcal{D}Q = \frac{1}{\pi^2} d\tilde{b} d\tilde{p} d\tilde{q} d\tilde{n} d\tilde{\zeta} d\tilde{\xi} d\tilde{\kappa} d\tilde{\omega} = \frac{4i}{\pi^2} du dv dw d\tilde{n} d\tilde{\zeta} d\tilde{\xi} d\tilde{\kappa} d\tilde{\omega}. \tag{3.14}$$

The integral with respect to the zero mode $\tilde{n}$ is taken analogously to the corresponding expression from (3.6): $\int d\tilde{n} = 2\pi|u - v|$. After integration with respect to $\tilde{n}$ and Grassmann variables, we obtain the following expression for the density of states:

$$\langle \rho \rangle = \frac{c_1 \tilde{G}^2}{4\pi\delta} \times \mathrm{Re} \int du dv dw |u - v|(u + w)(v + w)(u + v + 2w) \times \exp\left[-\tilde{G}\left(\tilde{\varepsilon}(u + v - 2w) - \frac{u^3 + v^3 - 2w^3}{3}\right)\right]. \tag{3.15}$$

Let us carry out the scaling transformation of the integration variables with a view to eliminate $\tilde{G}$: $(u, v, w) \longrightarrow (2\tilde{G})^{-1/3}(u, v, w)$, and pass to new variables $l = (u + v)/2$ and $m = (u - v)^2/2$. This leads to

$$\langle \rho \rangle = \frac{1}{8\pi^2 \Delta_g} \mathrm{Re} \int_0^\infty dm \times \int dl dw (w + l)(w^2 + 2lw + l^2 - m) \times \exp\left[-\frac{w^3}{3} + \epsilon w + \frac{l^3}{3} + ml - \epsilon l\right], \tag{3.16}$$

where

$$\epsilon = (2\tilde{G})^{2/3}\tilde{\varepsilon} = \frac{E_g - E}{\Delta_g}, \quad \Delta_g = \frac{c_2^{1/3}(\delta^2 E_g)^{1/3}}{2\pi^{2/3} c_1}. \tag{3.17}$$

At this stage, we must choose the contours of integration with respect to w and l. Integral (3.16) converges if the contours of integration with respect to l and w tend to infinity in hatched and light regions, respectively (see Fig. 4). This, however, is valid only when we can confine our analysis to the third-order terms in w and l in the expansion of action. In a region far from zero, convergence is determined by the properties of expression (2.31): the contour for w must tend to infinity along the imaginary axis (compactness of the FF sector), while the contour for l, along the real axis (noncompactness of the BB sector). Nevertheless, the main contribution to the integral comes from a neighborhood of zero; consequently, we will take this integral with a cubic action within infinite limits by displacing the contour for w to the left (C_1 in Fig. 4). For l, we have two alternatives: C_2 and C_3. A correct choice is determined by the condition of positiveness of the density of states, which corresponds to contour C_3 for l.

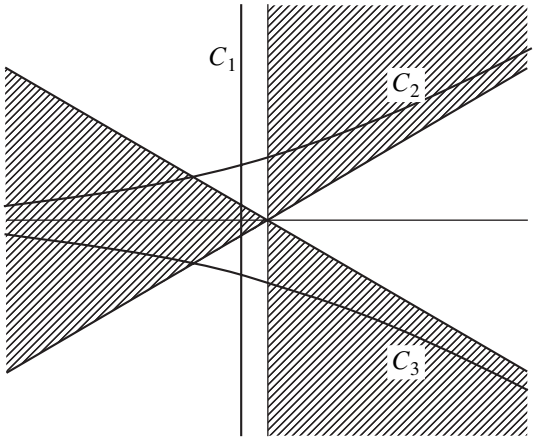

Fig. 4. Possible contours of integration with respect to w and l. Correct choice corresponds to C_1 for w and C_3 for l.

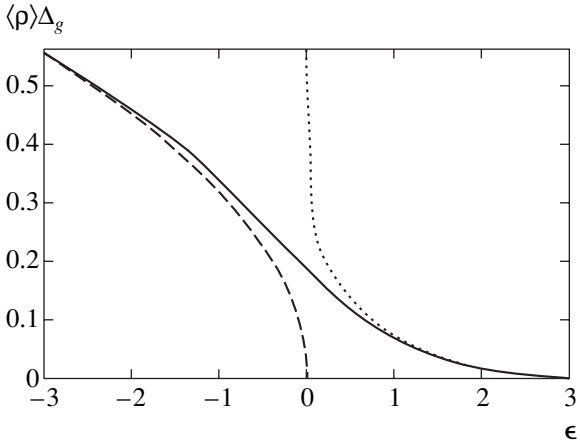

Fig. 5. Exact dependence (3.18) of the density of states $\langle\rho\rangle$ (in units of $1/\Delta_g$) on reduced energy ϵ (3.17) (solid curve). The size of the fluctuation region is on the order of unity. The asymptotic form of the density of states above the gap is given by expression (3.8) (dashed curve) and below the gap, by expression (3.7) (dotted curve).

Integral (3.16) is evaluated in Appendix B. The result of calculation is the following expression for the density of states,

$$\langle \rho \rangle = \frac{1}{\Delta_g}\left[-\epsilon \mathrm{Ai}^2(\epsilon) + [\mathrm{Ai}'(\epsilon)]^2 + \frac{\mathrm{Ai}(\epsilon)}{2}\left(1 - \int_\epsilon^\infty dy \mathrm{Ai}(y)\right)\right], \tag{3.18}$$

where ϵ is defined by the expression from (3.17). This dependence is depicted in Fig. 5 together with the asymptotic forms of relations (3.8) and (3.7).

The single-instanton approximation is valid in the limit $\epsilon \gg 1$. If we substitute into formula (3.18) the asymptotic expression for the Airy function,[5] the first two terms in the brackets cancel out and the integral is found to be much smaller than unity. As a result, Eq. (3.18) exactly coincides with expression (3.7).

Functional dependence (3.18) coincides with the predictions (formula (3.21) below) of the random matrix theory for the spectral edge in the case of an orthogonal ensemble [32]. Such a coincidence is not surprising in view of the equivalence of the random matrix theory and the zero-dimensional σ model [26]. In the case under investigation, the σ model becomes zero-dimensional in the vicinity of the threshold at the stage of introducing quasi-zero-dimensional variables (3.11) with a fixed coordinate dependence specified by function f_0. The application of the random matrix theory for NS systems will be discussed in greater detail in Subsection 3.3.

The results of this and preceding subsections are valid in the case when the normal region has an arbitrary shape and is linked via ideal contacts to an arbitrary number of superconductors with identical phases (see Fig. 3). It is only necessary that the approximation of the zero-dimensional σ model be satisfied. The criterion determining the effective dimensionality of the problem in an important special case of a planar SNS junction will be formulated in Subsection 5.1.

3.3. Method of Random Matrices

The random matrix theory was proposed by Wigner [17] in 1951 for describing properties of nuclear spectra. The idea of this theory is that the statistical properties of the spectrum of a complex and unknown nuclear Hamiltonian do not change upon replacement of all matrix elements by random numbers. Dyson [18] and Mehta [19] subsequently developed the random matrix theory.

In the simplest case, the random matrix theory is formulated for so-called Gaussian ensembles, for which the Hermitian random $N \times N$ matrix H acquired the statistical weight,

$$\mathcal{P}(H) \propto \exp\left(-\frac{\pi^2}{2N\delta^2}\mathrm{tr}H^2\right). \tag{3.19}$$

The average density of states for distribution (3.19) in the limit $N \longrightarrow \infty$ has the form of a Wigner semicircle,

$$\langle \rho(E)\rangle_{RMT} = \frac{1}{\delta}\sqrt{1-\frac{\pi^2E^2}{4N^2\delta^2}}, \tag{3.20}$$

vanishing for $|E| > E_0 \equiv (2/\pi)N\delta$. In accordance with the random matrix theory, the statistical properties of the spectrum at the center of the band for $|E| \ll E_0$ are determined only by the mean level spacing δ and by the symmetry of Hamiltonian H (orthogonal, unitary, or symplectic [19]).

In 1965, Gor'kov and Éliashberg [33] suggested that the random matrix theory may be applied for describing the statistical properties of energy levels in disordered metallic grains. However, the theory remained phenomenological up to 1982, when Efetov [21] used the supermatrix σ model for computing a pair correlator $R_2(\omega) = \delta^2\langle\rho(E)\rho(E+\omega)\rangle$ of energy levels for a metallic grain and proved that it coincides with the predictions of the random matrix theory in the zero-dimensional limit $\omega \ll E_{Th}$. Subsequently, the universality hypothesis, according to which local spectral properties of random systems near the center of a band are determined only by the symmetry of the Hamiltonian and not by its microscopic properties, was proved for a wide class of ensembles of random matrices [34].

In 1997, Altland and Zirnbauer [35] proposed a generalization of three standard Wigner–Dyson ensembles to the case of mixed NS systems by introducing four more symmetry classes, which take into account the mirror symmetry of the Bogoliubov–De Gennes equations. However, they confined analysis only to systems in which the average phase factor $\langle e^{i\phi}\rangle = 0$, where ϕ is the electron phase gained due to Andreev reflection processes. Such a situation is realized, for example, in the core of a superconducting vortex or in an SNS junction with a phase difference of π. Under such a condition, the proximity effect does not lead to the formation of a gap in the spectrum of the normal region, but specific superconducting correlations may appear for energies very close to the Fermi energy (at "distances" on the order of δ).

If, however, the superconducting order parameter averaged over the system does not vanish, the density of states is suppressed to zero on the Fermi surface, and a gap is formed for $E = E_g$ (in the semiclassical approximation). The states emerging near the gap cannot be described with the help of the random matrix theory at the center of the Wigner semicircle (3.20) even if we use new symmetry classes [35]. In 2001, Vavilov *et al.* [22] paid attention to the fact that the semiclassical density of states in NS systems near the threshold, as well as the density of states for a Wigner semicircle, exhibits identical (root) dependences on the distance to the threshold. They were the first to propose, in this connection, using the random matrix theory at the spectral

[5] The asymptotic form of the Airy function for $x \longrightarrow \infty$ has the form $\mathrm{Ai}(x) \sim \frac{1}{2\sqrt{\pi}x^{1/4}}e^{-2x^{3/2}/3}$.

edge for describing close-to-threshold states in NS systems.

The Wigner semicircle (3.20) describes the average density of states far away from thresholds $\pm E_0$. Corrections to it become significant at a distance of a single energy level from the threshold, i.e., for $|E| - E_0 \sim \Delta_0$, where $\Delta_0 = (\delta^2 E_0/2\pi^2)^{1/3}$. In the forbidden gap $|E| > E_0$, a nonzero average density of states appears; in this case,

$$\int_{E_0}^{\infty} \langle \rho(E) \rangle dE \sim 1,$$

which means that almost the entire density of states outside the Wigner semicircle is ensured by fluctuations of the position of the lowest energy level. Universal properties of the spectrum of random matrices near its edge were investigated in [32]. In particular, the exact profile of the average density of states near the threshold $E = E_0$ assumed the universal form in terms of the dimensionless quantity $x = (E - E_0)/\Delta_0$:

$$\langle \rho(E) \rangle = \frac{1}{\Delta_0}\left[-x\mathrm{Ai}^2(x) + [\mathrm{Ai}'(x)]^2 + \delta_{\beta,1}\frac{\mathrm{Ai}(x)}{2}\left(1 - \int_x^{\infty} dy\,\mathrm{Ai}(y)\right)\right], \quad (3.21)$$

where $\beta = 1$ or 2 for the orthogonal (unitary) class of symmetry.

The applicability of the random matrix theory for describing the edge of the spectrum in an NS system was proved for the first time in [30] with the help of the method of the supermatrix σ model. In the limit of the zero-dimensional σ model, which is valid in a close neighborhood of the threshold, we derived expression (3.18), exactly coinciding with result (3.21) obtained for the orthogonal symmetry.

4. CONTACT WITH TUNNEL INTERFACES

In this section, we consider an NS contact (Fig. 3) with nonideal boundaries. As the transparency of the interface decreases, quasiparticles stay for a longer time in the normal region between two Andreev reflections; accordingly, the gap in the density of states becomes smaller. In the tunnel limit, when the transparency of each channel between superconductors and the normal part of the contact is low, a gap is formed at energy $E_g = G_T\delta/8\pi$. In the vicinity of E_g, the semiclassical density of states vanishes in accordance with the law $\sqrt{|\varepsilon|}$; as the distance from the threshold increases, it attains its maximum value and then decreases in accordance with the law $1/\sqrt{|\varepsilon|}$ (see Eq. (4.30) below), resembling more and more a BCS-type singularity.

The shape of the tail in this case also changes, but the total number of quasi-localized states remains on the order of unity as before. The pattern changes qualitatively for $G_T \ll G^{1/4}$ (where G is the characteristic conductance of the normal part of the contact, which will be defined rigorously below). In this limit, the average number of energy levels in the region of the root increase in the density of states above energy E_g is on the order of unity, so that the entire region falls to the domain of strong fluctuations. The number of subgap states starts increasing simultaneously. This regime, which will be referred to as an strong tail, will be considered in Subsection 4.4.

4.1. Action for the Boundary

If the interface between a superconductor and a normal metal is ideal, matrix Q is continuous upon a transition from one region to another. If, however, the interface is not ideal, the boundary conditions become more complicated [36, 37]. These conditions can be taken into account automatically if we supplement the action of the σ model with an additional boundary term. It has the form [26, 38]

$$\mathcal{S}_{\text{boundary}} = -\frac{1}{4}\sum_i N_i \mathrm{str}\ln\left[1 - \frac{\Gamma_i}{2} + \frac{\Gamma_i}{4}\{Q, Q^{(i)}\}\right]. \quad (4.1)$$

Index i labels superconductors in contact with the normal region, and N_i is the total number of conducting channels in the ith contact per spin component. For a boundary of area S, the number of channels is $N = \pi\nu v_0 S$, where v_0 is the Fermi velocity; Γ_i is the transparency of a channel, which is assumed for simplicity to be identical for all the channels at the given interface; $Q^{(i)}$ is the value of matrix Q in the normal region in the vicinity of the ith contact; and Q_S is the value of matrix Q in the superconductor. Expression (4.1) can be used only if matrix $Q^{(i)}$ is constant along each interface. This condition is satisfied automatically for a planar SNS junction (see Fig. 1); in the general case (see Fig. 3), we must require that the size of the contacts is small as compared to the characteristic size of the normal region.

In our parametrization, the separation of variables (2.30) is preserved as before and the expression for S_0 acquires an additional term,

$$S_0[\theta] = \frac{\pi\nu}{4}\int d\mathbf{r}[D(\nabla\theta)^2 + 4iE\cos\theta] - \frac{1}{2}\sum_i N_i \ln(1 + \gamma_i \sin\theta^{(i)}), \quad (4.2)$$

where $\gamma_i = \Gamma_i/(2 - \Gamma_i)$. Here, $\theta^{(i)}$ is the value of angle θ in the normal region in the vicinity of the ith contact. It

was noted above that this value is independent of the coordinates along the boundary. This allows us to use the coordinate representation for the first term in the action and the channel representation for the second term. Henceforth, we will use the superscript "*i*" for values of various fields in the vicinity of the *i*th contact.

The entire classification of instantons made in Subsection 2.4 is preserved. In the expansion in fluctuations, we must supplement action (2.44) with the boundary term:

$$\mathcal{S}^{(2)}[W] = \frac{\pi\nu}{8} \times \int d\mathbf{r}\,\mathrm{str}\Big[D(\nabla W)^2 + \frac{D}{4}[\nabla U_0, W]^2 - 2iE\Lambda Q_0 W^2\Big] + \frac{1}{4}\sum_i N_i T_i \mathrm{str}\Big(\frac{\tau_x Q_0}{1 + T_i\tau_x Q_0}\tilde{W}^{(i)}\frac{1}{1 + T_i\tau_x Q_0}\tilde{W}^{(i)}\Big). \tag{4.3}$$

Here, we have introduced the notation $\tilde{W} = e^{-iU_0/2}We^{iU_0/2}$ and $T_i = (2 - \Gamma_i - 2\sqrt{1-\Gamma_i})/\Gamma_i = \gamma_i - 2\sqrt{1-\gamma_i^2}/\gamma_i$. Parametrization of W diagonalizing this action remains unchanged (Appendix A), but operator $\hat{\mathbb{O}}^{\pm}_{\alpha\beta}$ also acquires a boundary term:

$$(a\hat{\mathbb{O}}^{\pm}_{\alpha\beta}b) = \frac{\pi\nu}{8}\int d\mathbf{r}\Big[D(\nabla a(\mathbf{r}))(\nabla b(\mathbf{r})) - a(\mathbf{r})\Big(\frac{D}{4}(\nabla\alpha \pm \nabla\beta)^2 + iE(\cos\alpha + \cos\beta)\Big)b(\mathbf{r})\Big] + \sum_i \frac{N_i\gamma_i}{16} \times \Bigg(a^{(i)}\frac{(\sin\alpha^{(i)} + \sin\beta^{(i)}) + \gamma_i(1 \mp \cos(\alpha^{(i)} \pm \beta^{(i)}))}{(1 + \gamma_i\sin\alpha^{(i)})(1 + \gamma_i\sin\beta^{(i)})}b^{(i)}\Bigg). \tag{4.4}$$

Thus, the inclusion of nonideality of the boundary does not basically change the strategy of calculating the density of states near the threshold. We can repeat all calculations made for an ideal boundary in Section 3, taking into account the boundary term in the action. The only difference will be redefinition of functions $\psi_{1,2}$ and f_0 as well as constants $c_{1,2}$. The new definitions have the form

$$D\nabla^2\psi + 2E\cosh\psi = 0,\qquad D\nabla_n\psi^{(i)} + \gamma_i\nu_0\frac{\sinh\psi^{(i)}}{1 + \gamma_i\cosh\psi^{(i)}} = 0; \tag{4.5}$$

$$D\nabla^2 f_0 + 2E_g f_0\sinh\psi_0 = 0,\qquad D\nabla_n f_0^{(i)} + \gamma_i\nu_0 f_0^{(i)}\frac{\gamma_i\cosh\psi_0^{(i)}}{(1 + \gamma_i\cosh\psi_0^{(i)})^2} = 0; \tag{4.6}$$

$$c_1 = \frac{1}{V}\int d\mathbf{r}\, f_0\cosh\psi_0; \tag{4.7}$$

$$c_2 = \frac{1}{V}\int d\mathbf{r}\, f_0^3\cosh\psi_0 - \frac{\delta}{2\pi E_g} \times \sum_i N_i\gamma_i\sinh\psi_0^{(i)}\frac{1 - \gamma_i^2 - \cosh\psi_0^{(i)}}{(1 + \gamma_i\cosh\psi_0^{(i)})^3}[f_0^{(i)}]^3. \tag{4.8}$$

With these definitions, the results obtained in Subsections 3.1 and 3.2 are preserved.

It should be recalled once again that all formulas in this subsection are valid only when functions $\psi_{1,2}$ and f_0 are constant at the boundaries with a superconductor.

4.2. Zero-Dimensional Action

Here, we consider the case when the gradient terms in action (4.2) have the meaning of a small correction. Such a situation takes place either in the limit of tunnel contacts $\Gamma \approx 2\gamma \ll 1$, or for contacts whose size is smaller (Fig. 3) than the mean free path: $S_i \ll l^2$. In the latter case, diffusion in the normal part of the contact is not necessarily required; the mean free path can be on the order of the size of the system. Taking into account the gradient terms as a small correction, we can determine the optimal coordinate dependence $\psi(\mathbf{r})$ and obtain a zero-dimensional action.

Thus, if $\psi(\mathbf{r})$ changes in space insignificantly, we can single out a large constant,

$$\psi = A + \phi(\mathbf{r}), \tag{4.9}$$

and expand action (4.2) into a series up to the first order in ϕ and to the second order in $\nabla\phi$; in addition, we expand the logarithm in the action up to the second order in $\gamma\cosh A$ (omitting an insignificant constant). The validity of the inequality $\gamma\cosh A \ll 1$ will be proved below:

$$S_0[\psi] = \frac{\pi E}{\delta}\sinh A - \frac{G_T}{8}\cosh A + \frac{\pi\nu}{4}\int d\mathbf{r}(-D(\nabla\phi)^2 + 4E\phi\cosh A) + \frac{1}{4}\Big(\sum_i N_i\gamma_i^2\Big)\cosh^2 A - \frac{1}{2}\sum_i N_i\gamma_i\phi^{(i)}\sinh A, \tag{4.10}$$

where we have introduced the total tunnel conductance

of the contacts,

$$G_T = 2\sum_i N_i\Gamma_i \approx 4\sum_i N_i\gamma_i. \quad (4.11)$$

Disregarding the terms in the second and third lines in Eq. (4.10) and varying the action in A, we obtain $8\pi E/(G_T\delta) = \tanh A$. The effect of the omitted terms becomes significant for large values of A; in this case, corrections to $\tanh A$ are negative. This ensures the emergence of a peak in the dependence of energy on A, which determines the gap width. In the first approximation, we can assume that

$$E_g = \frac{G_T\delta}{8\pi}. \quad (4.12)$$

In the framework of the approximation used by us here, we can replace energy E in the fourth term in Eq. (4.10) by E_g. Using also the fact that A is large, we can replace the hyperbolic functions of A in the second and third lines of Eq. (4.10) by $P/2$, where $P = e^A$. As a result, we obtain action in the form

$$S_0[P,\phi] = -\frac{G_T}{16}\left[\varepsilon P + \frac{2}{P}\right] + \frac{P^2}{16}\sum_i N_i\gamma_i^2 + \frac{\pi\nu}{4}\int d\mathbf{r}\left(-D(\nabla\phi)^2 + \frac{G_T\delta}{4\pi}P\phi\right) - \frac{P}{4}\sum_i N_i\gamma_i\phi^{(i)}. \quad (4.13)$$

We have also introduced here the dimensionless energy measured from the edge of the gap:

$$\varepsilon = \frac{E_g - E}{E_g} = 1 - \frac{8\pi E}{G_T\delta}. \quad (4.14)$$

Varying the obtained action with respect to ϕ, we obtain the following equations:

$$D\nabla^2\phi + \frac{\delta G_T P}{8\pi} = 0, \qquad 2D\nabla_n\phi^{(i)} + P\nu_0\gamma_i = 0. \quad (4.15)$$

These equations define function ϕ to within a constant term since we have not fixed the constant in Eq. (4.9). For the sake of convenience, we introduce the function $\Phi(\mathbf{r}) = 2D\phi(\mathbf{r})/P\nu_0$, which has the dimension of length and satisfies the equations

$$V\nabla^2\Phi + \sum_i S_i\gamma_i = 0, \quad \nabla_n\Phi^{(i)} + \gamma_i = 0. \quad (4.16)$$

Here, S_i is the area of the ith contact. In such a form, the compatibility of the equation and the boundary conditions becomes obvious. Indeed, having integrating the first equation over the volume and applying the Gauss theorem, we obtain $\sum_i S_i(\nabla_n\Phi^{(i)} + \gamma_i) = 0$, which matches the boundary conditions on Eqs. (4.16).

Using Eqs. (4.16), we can simplify action (4.13), which becomes now a function of P only:

$$S_0(P) = -\frac{G_T}{16}\left[\varepsilon P + \frac{2}{P}\right] + \frac{P^2}{16}\sum_i N_i\gamma_i^2 + \frac{3\pi\nu\nu_0 P^2}{16l}\int d\mathbf{r}(\nabla\Phi)^2. \quad (4.17)$$

This expression indicates once again that the arbitrary constant in Φ is deprived of physical meaning. For subsequent calculations, we require only one quantity characterizing the geometry of the system and the properties of the junctions:

$$\tilde{\gamma} = \left(\sum_i S_i\gamma_i\right)^{-1}\left[\sum_i S_i\gamma_i^2 + \frac{3}{l}\int d\mathbf{r}(\nabla\Phi)^2\right]. \quad (4.18)$$

Let us consider some particular cases.

(i) **One-dimensional junction.** Let the normal region be a rectangle of length L (see Fig. 1) and be connected with two superconductors by identical junctions with a transparency of $2\gamma \ll 1$ (for each junction). In this case, the solution to Eq. (4.16) has the form $\Phi(x) = -\gamma x^2/L$, while parameter (4.18) becomes $\tilde{\gamma} = L\gamma/2l + \gamma \approx L\gamma/2l$. Thus, the first term in the square brackets in Eq. (4.18) can be neglected in comparison with the second term. If a superconductor is fixed only at one side, the corresponding parameter $\tilde{\gamma}$ becomes twice as large: $\tilde{\gamma} = L\gamma/l$.

(ii) **Two-dimensional junction.** If the normal region has the shape of a circle of radius R, bordering a superconductor, then $\Phi(r) = -\gamma r^2/2R$, and we ultimately have $\tilde{\gamma} = 3R\gamma/4l$.

(iii) **Three-dimensional junction.** Similarly, if the normal region has the shape of a sphere of radius R, function $\Phi(r)$ is the same as in the previous case and the result is $\tilde{\gamma} = 3R\gamma/5l$.

(iv) **Zero-dimensional junction.** By a zero-dimensional junction, we assume a normal metal of an arbitrary shape, connected to superconductors by narrow junctions (see Fig. 3). In this case, we can disregard the second term in the square brackets of Eq. (4.18) as compared to the first term; if all the channels have the same transparency Γ, we have $\tilde{\gamma} = \Gamma/2$. Indeed, if a junction has a shape similar to that depicted in Fig. 3, the main contribution to integral $\int d\mathbf{r}(\nabla\Phi)^2$ comes from regions in the vicinity of the superconductors. If the distance r from the ith junction with the superconductor is much larger than the contact size ($r \gg \sqrt{S_i}$), but much smaller than the size of the normal metal, we

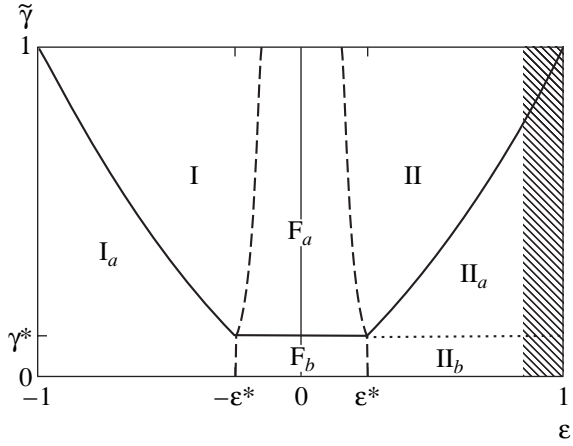

Fig. 6. Approximate "phase diagram" for possible energy dependences of the density of states. Formula (4.25) corresponds to regions I, (4.30) to I_a, (4.26) to II, and (4.44) to II_a and II_b. The density of states in regions I, F_a, and II is described by the universal formula (3.18) taking into account relations (4.24). The total number of prelocalized states in region II_b is large (see relation (4.46)). Parameters $\varepsilon^* = G^{-1/2}$ and $\gamma^* = G^{-3/4}$.

can approximately assume that $|\nabla\Phi| \approx S_i\gamma_i/2\pi r^2$. The integral of the square of this quantity is proportional to $S_i^{3/2}\gamma_i^2$ and can be disregarded in expression (4.18) provided that $S_i \ll l^2$.

The value of $\tilde{\gamma}$ depends on the geometry of the system and, in addition, is proportional to the "average" transparency of a channel in a junction. The tunnel conductance G_T is also proportional to the transparency of a channel. In order to analyze the behavior of various parameters of the system upon a change in the resistance of the junctions, we introduce a quantity describing the shape of the system only,

$$G = G_T/\tilde{\gamma}. \tag{4.19}$$

For a planar junction (see Fig. 1), it is proportional to the conductance of the normal part: $G = 12G_N$.

As a result, we obtain the zero-dimensional action

$$S_0(P) = \frac{G\tilde{\gamma}}{16}\left[-\varepsilon P - \frac{2}{P} + \frac{\tilde{\gamma}P^2}{4}\right]. \tag{4.20}$$

4.3. Classification of Tails

Here, we consider various limiting cases of variation of parameters $\tilde{\gamma}$ and ε, calculate the actions of instantons, and construct a rough pattern of possible behavior of the subgap density of states in various limiting cases.

By varying $S_0(P)$, we obtain the following equation[6] connecting P and ε:

$$\varepsilon = \frac{2}{P^2} + \frac{\tilde{\gamma}P}{2}. \tag{4.21}$$

The minimal value of ε is attained for $P = P_0 = 2\tilde{\gamma}^{-1/3}$ and is equal to $3\tilde{\gamma}^{2/3}/2 \ll 1$. This quantity has a nonzero value since the threshold energy E_g is in fact smaller than $G\tilde{\gamma}\delta/8\pi$. However, this correction is small and should be taken into account only while deriving the next formula.

For $E < E_g$, Eq. (4.21) has two real positive roots $P_{1,2}$ corresponding to two solutions $\theta_{1,2}$ to the Usadel equation. These roots can be found by expanding Eq. (4.20) in small parameters ε and $\delta P = P - P_0$:

$$S_0(P) = S_0(P_0) + \frac{G\tilde{\gamma}}{16}\left[-\varepsilon\delta P + \frac{2(\delta P)^3}{P_0^4}\right]. \tag{4.22}$$

Here, we have taken into account in ε the correction which was omitted in Eq. (4.14): $\varepsilon = 1 - 3\tilde{\gamma}^{2/3}/2 - 4\pi E/G\tilde{\gamma}\delta$. For our subsequent analysis, the accuracy of expression (4.14) is sufficient.

Expansion (4.22) leads to the conclusion that two solutions to the Usadel equation correspond to $P_{1,2} = P_0(1 \mp P_0\sqrt{\varepsilon/6})$, while the exponent for the density of states has the form

$$\mathcal{S} = S_0(P_1) - S_0(P_2) = \frac{G\tilde{\gamma}^{1/3}}{3\sqrt{6}}\varepsilon^{3/2}. \tag{4.23}$$

The same result can be obtained by comparing expansions (4.22) and (2.39). To this end, we must first establish the relation between g and δP. In the regime $\tilde{\gamma} \ll 1$, function $\psi_0(\mathbf{r})$ differs from a constant insignificantly; for this reason, in the main order, we can assume that $f_0(\mathbf{r}) \approx 1$. Thus, $\delta\psi = g$, and on the other hand, $\delta\psi = \delta\ln P = \delta P/P_0$. Equating the right-hand sides of Eqs. (4.22) and (2.39) termwise, we ultimately obtain

$$c_1 = \frac{P_0}{2} = \tilde{\gamma}^{-1/3}, \quad c_2 = \frac{6}{P_0} = 3\tilde{\gamma}^{1/3}, \quad \tilde{G} = \frac{3}{16}G\tilde{\gamma}^{4/3}. \tag{4.24}$$

If we substitute these constants into Eq. (2.41), we again arrive at result (4.23). Using expressions (4.24), we can generalize all results obtained in Subsections 3.1 and 3.2. In particular, for the density of states above the gap, we obtain from Eq. (3.8)

$$\langle\rho\rangle = \frac{1}{\tilde{\gamma}^{2/3}\delta}\sqrt{\frac{8|\varepsilon|}{3}}. \tag{4.25}$$

[6] For an ideal boundary, an analog of this equation was Eq. (2.6).

Similarly, we can determine the preexponential factor for the density of states under the gap from Eq. (3.7):

$$\langle\rho\rangle = \frac{1}{\delta}\sqrt{\frac{\pi}{G\tilde{\gamma}^{5/3}}\sqrt{\frac{2}{3\varepsilon}}}\exp\left(-\frac{G\tilde{\gamma}^{1/3}}{3\sqrt{6}}\varepsilon^{3/2}\right). \quad (4.26)$$

The last two formulas are valid outside the fluctuation region provided that $|\varepsilon| \gg G^{-2/3}\tilde{\gamma}^{-2/9}$, when we can disregard the contribution of the second instanton as compared to the first one. Figure 6 shows a rough "phase diagram" of possible behaviors of density of states for various values of $\tilde{\gamma}$ and ε. Formulas (4.25) and (4.26) correspond to regions I and II, respectively. Fluctuation region F_a lies between these regions. A universal expression for the density of states in the three regions (I, F_a, and II) can be obtained from Eq. (3.18) using Eq. (4.24) also.

Expansion (4.22) is valid if the energy differs from the threshold energy insignificantly. The validity of this expansion requires the fulfillment of inequality $|\delta P| \ll P_0$ or, which is the same, $|\varepsilon| \ll \tilde{\gamma}^{2/3}$.

In the opposite limit $\tilde{\gamma}^{2/3} \ll \varepsilon \ll 1$, the cubic parabola approximation (4.22) is inapplicable, and we must solve Eq. (4.21) to find $P_{1,2}$. In order to find the smaller root (P_1), we can disregard the last term, while the second root (P_2) can be found by disregarding the second term:

$$P_1 = \sqrt{\frac{2}{\varepsilon}}, \quad P_2 = \frac{2\varepsilon}{\tilde{\gamma}}. \quad (4.27)$$

Substituting these values into the expression for action (first part of relation (4.22)), we obtain

$$S_0(P_1) = -\frac{G\tilde{\gamma}}{4\sqrt{2}}\sqrt{\varepsilon}, \quad S_0(P_2) = -\frac{G\varepsilon^2}{16}. \quad (4.28)$$

Since $S_0(P_1) \ll S_0(P_2)$, the exponent for density of states is determined by $S_0(P_2)$ only:

$$\mathcal{S} = -S_0(P_2) = \frac{G\varepsilon^2}{16}. \quad (4.29)$$

The density of states with such an exponent corresponds to regions II_a and II_b. The preexponential factor for this regime will be obtained in the next subsection.

Formula (4.25) is also inapplicable in region I_a above the gap. In order to determine the density of states in this regime, we must solve Eq. (4.21) for a large negative ε. In order to find pairs of complex conjugate roots, we can disregard the last term in Eq. (4.21): $P_{1,2} = \pm i\sqrt{2/|\varepsilon|}$. In this case, density of states has the form

$$\langle\rho\rangle = \frac{2}{\delta}\mathrm{Re}\cos\theta = \frac{1}{\delta}\mathrm{Im}(P - P^{-1}) \approx \frac{1}{\delta}\sqrt{\frac{2}{|\varepsilon|}}. \quad (4.30)$$

Here, we have used root P_1 since the density of states must be positive.

As transparency $\tilde{\gamma}$ decreases, regions I and II become narrower and vanish when $\tilde{\gamma} \sim G^{-3/4}$. The single-instanton contribution to the density of states in this case is described only by an exponential function with exponent (4.29). It will be shown in Subsection 4.4 that the total number of subgap states increases as the value of $\tilde{\gamma}$ decreases below $G^{-3/4}$ (region II_b). Such a behavior will be referred to as an strong tail.

In the vicinity of the Fermi energy ($\varepsilon = 1$), a crossover to a non-zero-dimensional σ model takes place. The corresponding density of states will be considered in Subsection 5.3. This region is shaded in the figure.

It should be emphasized once again that a crossover from one dependence to another takes place near the boundaries of the regions, and the above formulas are valid only in the bulk of the corresponding region.

4.4. Strong Tail

Let us now consider the case when $\tilde{\gamma} \ll G^{-3/4}$. It corresponds to region II_b in Fig. 6. The density of state was determined with an exponential accuracy in the preceding subsection. We will determine now the preexponential factor.

The fluctuation region for the case under study is so large that the difference between functions ψ_1 and ψ_2 outside this region cannot be regarded as small, but their dependence on coordinates is still weak. While evaluating the Gaussian integral over hard modes, we obtain, as in Subsection 3.1, the factor

$$\sqrt{\frac{\det\hat{\mathbb{O}}^+_{\theta_1\theta_2}\det'\hat{\mathbb{O}}^-_{\theta_1\theta_2}}{\det\hat{\mathbb{O}}^+_{\theta_1\theta_1}\det'\hat{\mathbb{O}}^-_{\theta_1\theta_1}}} = \sqrt{\frac{(\mathscr{E}^+_{\theta_1\theta_2})_0}{(\mathscr{E}^+_{\theta_1\theta_1})_0}}, \quad (4.31)$$

where we have confined our analysis only to minimal eigenvalues of operators $\hat{\mathbb{O}}^+_{\theta_1\theta_2}$ and $\hat{\mathbb{O}}^+_{\theta_1\theta_1}$, since higher eigenvalues are mainly determined by the gradient term and exhibit a weak dependence on energy as before.

However, we will start with determining the quantities $(\mathscr{E}^-_{\theta_1\theta_1})_0$ and $(\mathscr{E}^-_{\theta_2\theta_2})_0$, which will be required anyway in subsequent analysis. For this purpose, we use relations (A.4) and formulas (2.30) and (4.20):

$$\frac{(\mathscr{E}^-_{\theta_1\theta_1})_0}{\delta} = \frac{1}{2}\frac{\partial^2\mathcal{S}}{\partial p^2} = -\frac{1}{4}\frac{\partial^2\mathcal{S}}{\partial\beta^2} \quad (4.32)$$

$$= \frac{1}{4}S_0''(P)\left(\frac{\partial P}{\partial\theta}\right)^2\Bigg|_{P=P_1} = \frac{G\tilde{\gamma}}{16}\left[\frac{1}{P_1} - \frac{\tilde{\gamma}P_1^2}{8}\right] = \frac{G\tilde{\gamma}}{16}\sqrt{\frac{\varepsilon}{2}}.$$

Analogous differentiation with respect to variable q gives

$$\frac{(\mathscr{E}^-_{\theta_2\theta_2})_0}{\delta} = -\frac{G\varepsilon^2}{32}. \tag{4.33}$$

The eigenvalue $(\mathscr{E}^-_{\theta_1\theta_2})_0$ corresponds to rotation of angle χ_B and is equal to zero. We will calculate $(\mathscr{E}^+_{\theta_1\theta_2})_0$ using perturbation theory. The corresponding eigenfunction differs insignificantly from a constant and can be set equal to unity:

$$\begin{aligned}(\mathscr{E}^+_{\theta_1\theta_2})_0 &= (1[\hat{\mathbb{O}}^+_{\theta_1\theta_2} - \hat{\mathbb{O}}^-_{\theta_1\theta_2}]1)\\ &= \frac{\pi\nu D}{8}\int d\mathbf{r}(\nabla\psi_1)(\nabla\psi_2)\\ &+ \sum_i \frac{N_i\gamma_i^2}{8}\cosh\psi_1^{(i)}\cosh\psi_2^{(i)} = \frac{\pi\nu\nu_0 P_1P_2}{32}\\ &\times\left[\frac{3}{l}\int d\mathbf{r}(\nabla\Phi)^2 + \sum_i S_i\gamma_i^2\right] = \frac{G\tilde{\gamma}}{32}\sqrt{\frac{\varepsilon}{2}}.\end{aligned} \tag{4.34}$$

Here, we have used expression (4.18) for $\tilde{\gamma}$.

In the same way, we can also calculate $(\mathscr{E}^+_{\theta_1\theta_1})_0$, but the perturbation theory correction to formula (4.32) obtained in this case will be small, so we can assume that

$$(\mathscr{E}^+_{\theta_1\theta_1})_0 = (\mathscr{E}^-_{\theta_1\theta_1})_0 = \frac{G\tilde{\gamma}}{16}\sqrt{\frac{\varepsilon}{2}}. \tag{4.35}$$

Thus, the contribution to the preexponential factor from hard fluctuations can be reduced to

$$\sqrt{\frac{(\mathscr{E}^+_{\theta_1\theta_2})_0}{(\mathscr{E}^+_{\theta_1\theta_1})_0}} = \frac{1}{\sqrt{2}}. \tag{4.36}$$

Subsequent calculations are similar to those from Subsection 3.1. Fluctuations of soft modes of variables b, p, and $\kappa\omega$ mutually cancel out, and we are left with an integral with respect to variables n, $\zeta\xi$, and q. The pair of Grassmann variables[7] ζ, ξ appears in the action in the form $\zeta\xi(\mathscr{E}^-_{\theta_1\alpha})_0/\delta$. In order to evaluate this eigenvalue (which differs from zero when $\alpha \neq \theta_2$), we will use the eigenfunction $\sinh((\psi_2-\psi_1)/2)$, which assumes, after normalization, the form

$$a(\mathbf{r}) = 1 + \frac{3(P_2-P_1)}{4l}\Phi(\mathbf{r}). \tag{4.37}$$

Substituting this expression into formula (4.4), using Eqs. (4.16) and (4.18), and carrying out cumbersome, but elementary transformations, we obtain

$$\begin{aligned}\frac{(\mathscr{E}^-_{\theta_1\alpha})_0}{\delta} &= \frac{G\tilde{\gamma}}{128}\frac{P_2+P_1}{P_2-P_1}\\ &\times\left[P_1\left(-\varepsilon + \frac{2}{P_1^2} + \frac{\tilde{\gamma}P_1}{2}\right) - P_2\left(-\varepsilon + \frac{2}{P_2^2} + \frac{\tilde{\gamma}P_2}{2}\right)\right].\end{aligned} \tag{4.38}$$

Here, P_2 stands not for the root of Eq. (4.21), but a variable parametrizing angle α: $\alpha \approx \pi/2 + i\ln P_2$. The quantity P_2 satisfies Eq. (4.21) only for $\alpha = \theta_2$; in this case, expression (4.38) obviously vanishes. The same was observed for ideal boundaries. At a saddle point, mode $\zeta\xi$ is zero, but its mass increases linearly upon a deviation in variable q. In our case, this corresponds to a deviation in P_2:

$$\delta P_2 = -iP_2\delta\alpha = -\frac{P_2}{\sqrt{2}}q. \tag{4.39}$$

Differentiating expression (4.38) with respect to P_2 (we must differentiate only the second term in the square brackets), we obtain

$$\frac{(\mathscr{E}^-_{\theta_1\alpha})_0}{\delta} = -\frac{G\tilde{\gamma}\varepsilon}{128}\delta P_2 = \frac{G\varepsilon^2 q}{64\sqrt{2}}. \tag{4.40}$$

Let us now calculate the preexponential factor in Eq. (2.24) in our approximation. Analogously to Eq. (3.4), we have

$$\begin{aligned}\frac{\nu}{4}\int d\mathbf{r}\,\mathrm{str}(k\Lambda Q) &= \mathrm{const} - \frac{\nu}{2}\delta\alpha\int d\mathbf{r}\cosh\psi_2\\ &= \mathrm{const} + \frac{i}{2\sqrt{2}\delta}\frac{\varepsilon q}{\tilde{\gamma}}.\end{aligned} \tag{4.41}$$

It remains for us only to determine the measure of integration with respect to variable n corresponding to the zero mode of rotation in angle χ_B. Using relations (A.4), we obtain, analogously to (3.6),

$$\begin{aligned}n &= 2i\sin k_B\chi_B = -2\sinh\frac{\psi_2-\psi_1}{2}\chi_B\\ &= -2\sqrt{\frac{P_2}{P_1}}\chi_B = -\frac{(2\varepsilon)^{3/4}}{\sqrt{2\tilde{\gamma}}}\chi_B,\\ \int dn &= \pi\sqrt{\frac{2}{\tilde{\gamma}}}(2\varepsilon)^{3/4}.\end{aligned} \tag{4.42}$$

[7] In Subsection 3.1, we used the notation $\zeta(\mathbf{r}) = \tilde{\zeta}f_0(\mathbf{r})$, etc., where the amplitude of fluctuations and their spatial profile are separated explicitly. In the limit we are dealing with now, the normalized eigenfunctions of operators $\hat{\mathbb{O}}$, corresponding to the lowest eigenvalues, differ from unity only slightly; consequently, we may not distinguish between $\tilde{\zeta}$ and ζ within the required accuracy.

We have now everything required for calculating the density of states. Using relations (4.33), (4.36), and (4.40)–(4.42), we obtain

$$\langle\rho\rangle = \frac{e^{-\mathcal{S}_0}}{\sqrt{2}}\mathrm{Re}\int\frac{dndq}{n}d\zeta d\xi\frac{i}{2\sqrt{2}\delta}\frac{\varepsilon q}{\tilde{\gamma}} \times \exp\left[\frac{G\varepsilon^2}{32}\left(q^2-\frac{q\zeta\xi}{2\sqrt{2}}\right)\right] = -\frac{2^{3/4}}{256\delta}G\frac{\varepsilon^{15/4}}{\tilde{\gamma}^{3/2}} \quad (4.43)$$

$$\times e^{-\mathcal{S}_0}\mathrm{Im}\int dq q^2\exp\left(\frac{G\varepsilon^2q^2}{32}\right).$$

Integrating along the imaginary axis, we finally obtain

$$\langle\rho\rangle = \frac{1}{\delta}\sqrt{\frac{\pi}{G\tilde{\gamma}^3}}\sqrt{\frac{\varepsilon^3}{8}}\exp\left(-\frac{G\varepsilon^2}{16}\right). \quad (4.44)$$

This result describes the behavior of density of states in regions II_a and II_b in Fig. 6. In region II_a, the obtained dependence is matched with Eq. (4.26) for $\varepsilon\sim\tilde{\gamma}^{2/3}$:

$$\langle\rho\rangle|_{\varepsilon\sim\tilde{\gamma}^{2/3}}\sim\frac{1}{\delta\sqrt{G\tilde{\gamma}}}\exp(-G\tilde{\gamma}^{4/3}). \quad (4.45)$$

Matching in region II_b is more complicated. The semiclassical density of states vanishes according to root law (4.25) at the boundary of the gap, attains its peak value for $|\varepsilon|\sim\tilde{\gamma}^{2/3}$, and then decreases in accordance with inverse root law (4.30). As the transparency of the boundary decreases, the size of the fluctuation region increases, and this region covers the peak of the density of states for $\tilde{\gamma}\sim G^{-3/4}$.

The density of states increases as we approach fluctuation region F_b on both sides; consequently, there must be no formal matching of these two dependences: the peak of the density of states lies in the fluctuation region.

Finally, let us estimate the total number of quasilocalized states:

$$\mathcal{N}\sim\int_0^1\frac{E_g d\varepsilon}{\delta\sqrt{G\tilde{\gamma}^3}}\varepsilon^{3/4}e^{-G\varepsilon^2}\sim\tilde{\gamma}^{-1/2}G^{-3/8}\gg 1. \quad (4.46)$$

Thus, for $\tilde{\gamma}\ll G^{-3/4}$, the number of states under the gap becomes large, which explains the term "strong tail" used in this case. These are apparently most suitable conditions for experimental verification of the above theory.

5. NONUNIVERSAL DENSITY OF STATES

In this section, we consider various cases in which density of states cannot be described by the zero-dimensional σ model. Subsection 5.1 deals with the situation when the instanton describing subgap states has a finite spatial size smaller than the size of the normal part of the contact. Fluctuations near such an instanton solution have a quasi-continuous spectrum, which considerably complicates the calculation of the preexponential factor in the density of states. For this reason, all results of this subsection (and the entire Section 5) will be obtained with an exponential accuracy.

In Subsection 5.2, the problem of subgap states in a superconductor with magnetic impurities is considered. In contrast to the rest of the material, it deals with a spatially homogeneous sample and not with a hybrid system. Quasi-localized states appear owing to spatial fluctuations of magnetic impurities. The problem of subgap states in such a system was solved in [23, 24]. The results are derived, and their relation with quasi-localized states in hybrid systems is demonstrated.

Subsection 5.3 is devoted to the density of states deep in the gap in the vicinity of the Fermi energy. This density of states cannot be described by the zero-dimensional σ model either and will be determined with an exponential accuracy.

5.1. Broad SNS Junction

This and the next subsections are devoted to analysis of a planar SNS junction (see Fig. 1). If the junction is long (the exact criterion will be formulated later), the results obtained in Subsections 3.1 and 3.2 are valid. It should be recalled that the corresponding numerical parameters have the following values in the given case: $c_1\approx 1.15$, $c_2\approx 0.88$, $E_g = 3.12E_{Th}$, and $\tilde{G} = \pi c_2 E_g/2\delta = 0.34G_N$. Here, $E_{Th} = D/L_x^2$ and $G_N = 4\pi\nu DL_yL_z/L_x = 4\pi E_{Th}/\delta$. In the case when the resistance of the contacts is finite, we can use values (4.24) (naturally, if $\varepsilon\ll\tilde{\gamma}^{2/3}$).

The action of an instanton defined by formula (2.41) is proportional to the conductance of the normal region and increases with its sizes in the *y* and *z* direction parallel to the NS interfaces. Consequently, for large values of L_y and L_z, it is more expedient to form an instanton with finite sizes along the *y* and *z* axes. In this case, a loss appears due to gradient terms, but it is compensated by the independence of action of the size of the normal region for large values of L_y and L_z. It will be shown below that the characteristic size of such a field configuration depends on the closeness to the threshold and is on the order of $L_\perp(E)\sim L_x\varepsilon^{-1/4}$.

We will calculate here the action of an instanton for a quasi-two-dimensional and three-dimensional contacts (one-dimensional and two-dimensional σ models, respectively), when one or both transverse sizes exceed $L_\perp(E)$, and obtain a result for the subgap density of states with an exponential accuracy. The power of energy in the exponent will differ from the case of a long one-dimensional junction.

In order to calculate the action for an instanton, we repeat the arguments leading to formula (2.39), but

assume that g is a function of transverse coordinates: $\theta = \pi/2 + i\psi_0(x) + ig(\mathbf{r}_\perp)f_0(x)$:

$$S_0[\theta] = \text{const} + \frac{\pi}{2\delta}\int\frac{dydz}{L_yL_z} \times\left[-\frac{D}{2}(\nabla_\perp g)^2 + E_g\left(-2c_1\varepsilon g + \frac{c_2}{3}g^3\right)\right]. \quad (5.1)$$

This action has two obvious saddle points $g = \pm\sqrt{\tilde{\varepsilon}}$ independent of the transverse coordinates, as in the case of the zero-dimensional problem. We retain for function θ_1 the solution $\theta_1 = \pi/2 + i\psi_0 - i\sqrt{\tilde{\varepsilon}}f_0$ and seek a solution for θ_2 as a function of transverse coordinates. For the sake of convenience, we introduce a function $\tilde{g}$ which describes the dependence of $\theta_2 - \theta_1$ on transverse coordinates and, in addition, transform the variables to the dimensionless form:[8]

$$g(\mathbf{r}_\perp) = \sqrt{\tilde{\varepsilon}}[2\tilde{g}(\tilde{\mathbf{r}}_\perp) - 1], \quad \tilde{\mathbf{r}}_\perp = \frac{\mathbf{r}_\perp}{L_\perp}, \quad L_\perp = \sqrt{\frac{D}{2c_2E_g}}\tilde{\varepsilon}^{-1/4}. \quad (5.2)$$

In this case, action assumes the form

$$\mathcal{S} = S_0[\theta_1] - S_0[\theta_2] = \frac{8L_\perp^2}{L_yL_z}\tilde{G}\tilde{\varepsilon}^{3/2} \times\int_0^{L_\perp/L_y}d\tilde{y}\int_0^{L_\perp/L_z}d\tilde{z}\left[\frac{(\tilde{\nabla}_\perp\tilde{g})^2}{2} + \frac{\tilde{g}^2}{2} - \frac{\tilde{g}^3}{3}\right]. \quad (5.3)$$

By varying this action, we obtain an equation for $\tilde{g}$, which describes the shape of an instanton in transverse directions:

$$\tilde{\nabla}_\perp^2\tilde{g} = \tilde{g} - \tilde{g}^2. \quad (5.4)$$

Substituting the expression for the Laplacian into the action again and integrating by parts, we finally obtain

$$\mathcal{S} = \frac{4}{3}\frac{L_\perp^2}{L_yL_z}\tilde{G}\tilde{\varepsilon}^{3/2}\int d\tilde{y}d\tilde{z}\tilde{g}^3(\tilde{y},\tilde{z}). \quad (5.5)$$

(i) **One-dimensional junction** ($L_{y,z} \ll L_\perp$). When the transverse sizes of the normal part of the junction are small, the results obtained in Section 3 are valid. In this case, $\tilde{g} \equiv 1$, the integral in Eq. (5.5) is equal to $L_yL_z/L_\perp^2$, and we return to expression (2.41) or (4.23) (in the case of tunnel contact). In this limit, the approximation of the zero-dimensional σ model is applicable and, hence, our previous results (3.7) and (4.26) for tunnel contacts are valid.

[8] The value of $L_\perp$ determined in this way is half the value used in [29].

(ii) **Two-dimensional junction** ($L_z \ll L_\perp \ll L_y$). We must solve Eq. (5.4) under the condition that $\tilde{g}$ is a function of y only. This equation describes a soliton of the Korteweg–de Vries type; its solution is well known:

$$\tilde{g}(\tilde{y}) = \frac{3}{2\cosh^2(\tilde{y}/2)}. \quad (5.6)$$

Substituting $\tilde{g}$ into Eq. (5.5), we obtain the following expression for density of states:

$$\langle\rho\rangle \sim \frac{1}{\delta}\exp\left(-\frac{48}{5}\frac{L_\perp}{L_y}\tilde{G}\tilde{\varepsilon}^{3/2}\right) = \frac{1}{\delta}\exp(-4.67G_\square\varepsilon^{5/4}). \quad (5.7)$$

Here, the large dimensionless parameter in the exponent, which determines the applicability of the steepest descent method, is the dimensionless conductance per unit area of the film of the normal metal connecting the superconducting banks: $G_\square = 4\pi\nu DL_z$.

In the case of tunnel contacts, using Eq. (4.24), we obtain

$$\langle\rho\rangle \sim \frac{1}{\delta}\exp(-2.17G_\square\tilde{\gamma}^{-1/6}\varepsilon^{5/4}). \quad (5.8)$$

Here, $\tilde{\gamma} = L_x\Gamma/4l \ll 1$.

(iii) **Three-dimensional junction** ($L_\perp \ll L_{y,z}$). The two-dimensional equation (5.4) cannot be solved analytically. We can only give the numerical result for integral (5.5):

$$\int d\tilde{y}d\tilde{z}\tilde{g}^3(\tilde{y},\tilde{z}) \approx 46.5. \quad (5.9)$$

The density of states can be written in the form

$$\langle\rho\rangle \sim \frac{1}{\delta}\exp(-10.1G_\square\varepsilon). \quad (5.10)$$

In this formula, $G_\square$ denotes the dimensionless conductance per unit area of the film, oriented parallel to the superconducting banks: $G_\square = 4\pi\nu DL_x$.

For tunnel contacts, we obtain

$$\langle\rho\rangle \sim \frac{1}{\delta}\exp(-2.58G_\square\tilde{\gamma}^{-2/3}\varepsilon), \quad (5.11)$$

where $\tilde{\gamma} = L_x\Gamma/4l \ll 1$ as before.

The criterion determining whether or not the dependence of an instanton solution on a transverse coordinate should be taken into account is based on the comparison of $L_\perp$ and $L_{y,z}$. Since the quantity $L_\perp$ is itself a function of energy, dimensions are "frozen out" as we approach the threshold: a crossover occurs from the two-dimensional σ model to the one-dimensional and then to zero-dimensional model.

5.2. Superconductor with Magnetic Impurities

In this section, we consider quasi-localized states in a superconductor with magnetic impurities. In the given case, we are speaking of a macroscopically homogeneous system in contrast to all the cases considered above (and below). The method of nonlinear σ model for determining anomalously localized states in such a system was developed in [23, 24].

A superconductor with magnetic impurities was studied in detail in the mean field approximation in the famous work by Abrikosov and Gor'kov [28]. Among other things, they proved that superconductivity is suppressed by magnetic impurities, the order parameter Δ being larger than the gap E_g in the excitation spectrum. Thus, the gapless superconductivity regime is possible, when $E_g = 0$, while $\Delta > 0$. Following [23, 24], we will consider, however, the case of a finite gap and will determine the instanton correction to the density of states under the gap with an exponential accuracy.

The introduction of magnetic impurities requires a refining of the σ model. The Bogoliubov–De Gennes Hamiltonian now contains an additional term describing scattering at magnetic impurities:[9]

$$\mathcal{H} = \tau_z\left(\frac{\mathbf{p}^2}{2m} - \mu + U(\mathbf{r})\right) + \tau_x\Delta(\mathbf{r}) + J\mathbf{S}(\mathbf{r})\cdot\hat{\boldsymbol{\sigma}}. \quad (5.12)$$

Since magnetic impurities suppress superconductivity, the order parameter Δ appearing in Hamiltonian (5.12) should be determined self-consistently. We assume that the magnetic impurity concentration is quite low and does not destroy superconductivity completely. In all the formulas of this subsection, we assume that the effect of impurities has already taken into account in Δ.

We assume that the random field $\mathbf{S}(\mathbf{r})$ in Eq. (5.12) is delta-correlated and introduce the time τ_s of scattering by magnetic impurities in the standard manner:

$$\langle JS_\alpha(\mathbf{r})JS_\beta(\mathbf{r}')\rangle = \frac{\delta(\mathbf{r}-\mathbf{r}')\delta_{\alpha\beta}}{6\pi\nu\tau_s}. \quad (5.13)$$

Thus, our system has acquired another dimensionless parameter,

$$\zeta = \frac{1}{\tau_s\Delta}. \quad (5.14)$$

The derivation of the σ model is generalized in a trivial manner to the case of Hamiltonian (5.12). In this case, action assumes the form

$$\mathcal{S}[Q] = \frac{\pi\nu}{8}\int d\mathbf{r} \times \mathrm{str}\left[D(\nabla Q)^2 + 4iQ(\Lambda E + i\tau_x\Delta) - \frac{(Q\tau_z\boldsymbol{\sigma})^2}{3\tau_s}\right]. \quad (5.15)$$

Here, the diffusion coefficient is determined by scattering by nonmagnetic impurities only. The Usadel equation can be derived without introducing complete parametrization of matrix Q, but using a simple expression in terms of angle θ alone: $Q = \sigma_z\tau_z\cos\theta + \tau_x\sin\theta$. Separating, as usual, the imaginary part $\theta = \pi/2 + i\psi$, we obtain

$$D\nabla^2\psi + 2E\cosh\psi - 2\Delta\sinh\psi + \frac{1}{\tau_s}\sinh 2\psi = 0. \quad (5.16)$$

Let us first consider homogeneous solutions to this equation. As before, we have two such solutions for energies below a certain threshold E_g. Omitting the gradient term, we can write the equation in a form resembling Eq. (2.6):

$$\frac{E}{\Delta} = \tanh\psi - \zeta\sinh\psi. \quad (5.17)$$

This equation has two solutions. The energy for which these solutions coincide determines the gap width. The maximum of the function on the right-hand side is attained for $\cosh\psi = \zeta^{-1/3}$, which corresponds to

$$E_g = \Delta(1-\zeta^{2/3})^{3/2}. \quad (5.18)$$

This remarkable result was obtained for the first time in [28].

In the vicinity of the threshold, we can expand the action in the dimensionless energy $\varepsilon = (E_g - E)/\Delta$ and in the deviation of the angle $\psi = \psi_0 + g(\mathbf{r})$. As a result, we obtain the following action for $g(\mathbf{r})$:

$$S_0[\theta] = \frac{\pi\nu\Delta}{4}\int d\mathbf{r} \times [\xi^2(\nabla g)^2 + 4\varepsilon\zeta^{-1/3}g - 2\zeta^{1/3}\sqrt{1-\zeta^{2/3}}g^3]. \quad (5.19)$$

Here, we have introduced the coherence length $\xi = \sqrt{D/\Delta}$. The obtained action is completely analogous to expression (5.1). Thus, subsequent calculations just repeat the preceding subsection and lead to the following result [23, 24]:

$$\langle\rho\rangle \sim \delta^{-1}\exp\left[-\frac{16}{3}a_d\pi\nu^{(d)}\Delta\xi^d\zeta^{-2/3} \times (24\sqrt{1-\zeta^{2/3}})^{-(2+d)/4}\varepsilon^{(6-d)/4}\right]. \quad (5.20)$$

Here, d is the effective spatial dimension of the superconductor, $\nu^{(d)}$ is the d-dimensional density of states,

[9] The symbol $\hat{\boldsymbol{\sigma}}$ for the electron spin operator is supplied with a hat to distinguish it from the Pauli spin matrices σ_i acting in the PH space. The spin operator can be expressed in terms of Pauli matrices as $\hat{\boldsymbol{\sigma}} = \tau_z\boldsymbol{\sigma}$.

and the quantity $a_d = \int d^d\mathbf{r}\tilde{g}^3$ was evaluated in Subsection 5.1 (function $\tilde{g}$ satisfies the equation $\nabla^2\tilde{g} = \tilde{g} - \tilde{g}^2$). This quantity assumes the following values:

$$a_0 = 1, \quad a_1 = 36/5, \quad a_2 \approx 46.5, \quad a_3 \approx 262. \quad (5.21)$$

5.3. Low-Energy Limit

In this subsection, we consider the range of energies close to the Fermi energy. For such energies, the density of states is suppressed the most strongly. As before, we will seek a solution with an exponential accuracy; for this purpose, we must solve the Usadel equation (2.2) and calculate action (2.30) based on the solution.

Our calculations almost repeat the calculations made by Muzykantskii and Khmelnitskii [39] (see also [40, 41]), who applied the instanton method in the diffusive σ model for determining the long-time asymptotic form of conductance $G(t)$ of a mesoscopic sample. The saddle equation appearing in this case and describing the instanton solution has the form $D\nabla^2\theta + i\omega\sinh\theta = 0$ with the boundary condition $\theta = 0$, where the quantity ω defined by the self-consistency equation [39] is inversely proportional to t. In the limit $\omega \ll E_{Th}$, the nontrivial solution of this equation almost coincides with solution ψ_2 to Eq. (2.5) for an SNS junction for $E \ll E_{Th}$. As a result, the actions of instantons in our problem and in the problem solved in [39] turn out to be identical.

We begin with a long planar SNS junction (see Fig. 1). The difference $\psi_2 - \psi_1$ is not small for energies $E \longrightarrow 0$; consequently, we must solve Eq. (4.5) directly. It should be noted that, as the energy decreases, $\psi_1(0) \longrightarrow 0$, while $\psi_2(0) \longrightarrow \infty$ (see Fig. 2). This enables us to set $\psi_1 = 0$ and to use the "triangular" approximation for ψ_2 [39],

$$\psi_2(x) = A + B\left(1 - \frac{2|x|}{L_x}\right), \quad (5.22)$$

which is based on the assumption that, for low energies, we can disregard the second term in Eq. (4.5) almost in the entire range of x except in the vicinity of zero. Substituting expression (5.22) into action (4.2), integrating, and expanding the boundary logarithm, we obtain

$$S_0 = \frac{\pi\nu D L_y L_z}{L_x} \times\left[-B^2 + \frac{E}{BE_{Th}}(\cosh(A+B) - \cosh A) - 6\tilde{\gamma}\cosh A\right]. \quad (5.23)$$

Let us first consider ideal boundaries, for which we can set $A = 0$. Carrying out the variation in B (considering that $B \gg 1$), we obtain

$$2B = \frac{Ee^B}{2BE_{Th}}. \quad (5.24)$$

To a logarithmic accuracy, we obtain the following equation for B:

$$B = \ln\frac{E_{Th}}{E} = \ln\frac{E_g}{E}. \quad (5.25)$$

Substituting this result back into Eq. (5.23), we find the density of states,

$$\langle\rho\rangle \sim \frac{1}{\delta}\exp\left(-\frac{G_N}{4}\ln^2\frac{E_g}{E}\right), \quad (5.26)$$

where $G_N = 4\pi\nu D L_y L_z/L_x$.

In the case of tunnel boundaries between a normal metal and superconductors, we must vary Eq. (5.23) in both variables in the limit $A, B \gg 1$. This gives

$$e^B = 6\tilde{\gamma}\frac{E_{Th}}{E}B = \frac{E_g}{E}B, \quad e^{A+B} = \frac{4E_{Th}}{E}B^2. \quad (5.27)$$

Here, we have used the equality $E_g = 6\tilde{\gamma}E_{Th}$. To a logarithmic accuracy, we obtain the following solution:

$$B = \ln\frac{E_g}{E}, \quad e^A = \frac{2}{3\tilde{\gamma}}\ln\frac{E_g}{E}. \quad (5.28)$$

In view of the smallness of E/E_g and $\tilde{\gamma}$, the first term in action (5.23) predominates. In this case, the density of states has form (5.26), as for a contact with ideal boundaries. This is not surprising, since strongly localized states, which are linked to the superconducting banks very weakly, lie deep in the gap. The density of such states exhibits a weak dependence on the properties of the boundary.

For low energy values, the result obtained becomes inapplicable. As a matter of fact, the gradient of ψ_2 tends to infinity, and the diffusion equation forming the basis of the σ model disregards nonlocal (ballistic) effects which become important in this case. The applicability of the local theory requires the fulfillment of the condition $|\nabla\psi_2| \sim B/L_x \ll 1/l$, setting a limit on the energy:

$$E \gg E_g\exp\left(-\frac{L_x}{l}\right). \quad (5.29)$$

Let us now consider the two-dimensional case. For the sake of simplicity, we assume that the normal region has the shape of a disc of radius R and thickness L_z, connected to a superconductor along the entire boundary. As in the previous example, $\psi_1 = 0$. We write Eq. (4.5) for ψ_2 in polar coordinates, assuming that the

radius is equal to unity and replacing the hyperbolic cosine by the exponential:[10]

$$\psi_2'' + \frac{\psi_2'}{r} + \frac{E}{E_{Th}} e^{\psi_2} = 0, \quad \psi_2'(0) = 0. \tag{5.30}$$

This equation has the following solution:

$$\psi_2(r) = 2\ln\frac{B\sqrt{8E_{Th}/E}}{B^2 + r^2}, \tag{5.31}$$

where B must be chosen from the boundary condition in (4.5).

If the boundary between the superconductor and the normal metal is transparent, we must require that $\psi_2(1) = 0$. For $E \ll E_{Th}$, we obtain $B = \sqrt{E/8E_{Th}}$. As before, disregarding the term with energy in Eq. (2.31), we obtain the following expression for action:

$$\mathcal{S} = -S_0[\theta_2] = \frac{\pi\nu D}{4} R^2 L_z \times \int\limits_{\sqrt{E/E_g}}^{1} (\nabla\psi_2)^2 2\pi r dr = 4\pi^2 \nu D L_z \ln\frac{E_g}{E}. \tag{5.32}$$

The density of states is a power function of energy [39]:

$$\langle\rho\rangle \sim \left(\frac{E}{E_g}\right)^{4\pi^2\nu D L_z} = \left(\frac{E}{E_g}\right)^{\pi G_\square}. \tag{5.33}$$

In the case of a tunnel boundary, replacing the hyperbolic sine in the boundary condition (4.5) by an exponential, we obtain

$$B = \frac{1}{2}\sqrt{\frac{E}{\tilde{\gamma}E_{Th}}} = \sqrt{\frac{E}{E_g}}. \tag{5.34}$$

In this equality, we have used the expression $E_g = 4\tilde{\gamma}E_{Th}$, which is valid in the two-dimensional case. Thus, result (5.33) remains valid to a logarithmic accuracy in the case of the tunnel boundary also; i.e., the resistance of the contacts does not affect the density of states lying deep in the gap as in the one-dimensional case.

For a two-dimensional SNS junction of a different shape, the results will have the same order of magnitude, since only E_g depends on the longitudinal size, and this will only change the general numerical factor in the expression for the density of states.

Let us determine the region of applicability of the result. The maximum gradient of ψ_2 is attained in the vicinity of the center, $|\nabla\psi_2| \propto \sqrt{E_g/E}/R$, and must be smaller than $1/l$. Thus, the power dependence of density of states is valid for

$$E \gg E_g\left(\frac{l}{R}\right)^2. \tag{5.35}$$

This condition is much more stringent than condition (5.29). In the three-dimensional case, the line of reasoning similar to that used in this subsection is completely impossible since the corresponding condition turns out to be too stringent. In this case, as well as in the two-dimensional case, the subgap density of states for energies lower than (5.35) can be found with the help of the ballistic σ model [42] (see also [43]).

It should be noted that, after the substitution $E \longrightarrow t_\phi^{-1}$, expressions (5.26) and (5.33) coincide (to within a factor) with the distribution function $\mathcal{P}(t_\phi)$ of the relaxation times for a corresponding mesoscopic system [44, 45]. The long-time asymptotic form of conductance can be expressed in terms of this distribution function as $G(t) \sim \int dt_\phi e^{-t/t_\phi}\mathcal{P}(t_\phi)$. Evaluating the integral by the steepest descent method, we obtain

$$G(t) \sim \exp\left[-\frac{G_N}{4}\ln^2(\delta t)\right],$$

for a one-dimensional system, which corresponds to the substitution $i\omega \longrightarrow G_N/t$ in the Muzykantskii–Khmelnitskii formalism. This explains the difference in the energy scales in our problem and in the problem on the asymptotic form of conductance. Results (5.26) and (5.33) are transformed to the asymptotic expressions [39] for $G(t)$ via the substitution $E_{Th}/E \longrightarrow \delta t$.

6. CONCLUSIONS

We have considered the density of quasiparticle states in diffusive NS systems for energies close to the semiclassical gap $E_g \ll \Delta$, appearing due to mesoscopic fluctuations.

For a system with ideal contacts, exact expression (3.18) for the averaged density of states is obtained in the framework of the zero-dimensional σ model with a large parameter $\tilde{G} \propto E_g/\delta \gg 1$ for energies E in the vicinity of $E_g \sim E_{Th} \sim D/L^2$. For $\varepsilon = (E_g - E)/E_g \geq \tilde{G}^{-2/3}$, the density of states decreases exponentially (see Eq. (3.7)), which resembles to a certain extent the behavior of density of states in semiconductors with impurities (the so-called Lifshits tail [13]). The total number of states in the tail region is found to be on the order of unity for a one-dimensional system; i.e., the equation obtained for density of states has the meaning of the probability of an anomalous location of the lower energy level below E_g. The results are in perfect agreement with the phenomenological random matrix theory [22] and make it possible to determine

[10] Here, $E_{Th} = D/R^2$.

the range of its applicability as well as the values of microscopic parameters used in it.

For planar SNS junctions with a large transverse size $L_{y,z} \geq L_x\varepsilon^{-1/4}$ (see Fig. 1), analogous results were obtained with an exponential accuracy (see relations (5.7) and (5.10)). In view of the large area of the contacts, the averaged (integrated) density of states has direct physical meaning in this case. The problem of the fluctuation tail of the density of states in a superconductor with a low concentration of magnetic impurities, which was considered for the first time in [23, 24], is also found to be formally similar.

Physical factors responsible for the emergence of low-lying electron states in our problem are mesoscopic fluctuations in the normal region of the contact, which lead to the diffusion electron–hole (Andreev) trajectories with a period larger than the characteristic diffusion time L^2/D. A similar effect is observed during analysis of asymptotic forms of the distribution functions for density of states, conductance, and relaxation times for normal systems [44]. Due to mesoscopic fluctuations of impurities, almost localized states can also be found with an exponentially low probability in the energy range corresponding to well delocalized states. Such states ensure an anomalously slow relaxation of current to its equilibrium value over very long times (larger than the inverse mean spacing νV); i.e., such states play the role of "electron traps." Naturally, such traps must appear in the problem of an NS system also, since it is these traps that lead to the emergence of trajectories diffusing between Andreev reflection for an anomalously long time. A direct relation between "anomalously localized states" and low-lying states in an SNS junction follows from our results for the density of states in the low-energy range $E \ll E_g$ (see relations (5.26) and (5.33) for one- and two-dimensional case, respectively). Upon the substitution $E \longrightarrow t_\phi^{-1}$, these formulas coincide (to within a normalization) with the distribution function for relaxation times t_ϕ of a mesoscopic system [39, 44, 45].

We have also considered hybrid NIS structures with a poor transparency of NS interfaces. Such systems can be described by two characteristic parameters: the total tunnel conductance G_T between the normal and superconducting parts and the effective average transparency $\tilde{\gamma}$ of a channel, which depends on the properties of the contacts and on the system geometry (see Eq. (4.18)). In the limit of a low effective transparency of a channel, $\tilde{\gamma} \ll 1$, the semiclassical edge of the spectrum is displaced towards low energies, $E_g = G_T\delta/8\pi$. The behavior of the density of states above the threshold simultaneously changes qualitatively: as the energy decreases, the density of states first increases as in the BCS theory, $\langle\rho(E)\rangle \propto |\varepsilon|^{-1/2}$, and starts decreasing in accordance with the law $\langle\rho(E)\rangle \propto \sqrt{|\varepsilon|}$ only for $|\varepsilon| < \tilde{\gamma}^{2/3}$.

In the limit $\tilde{\gamma} \ll G_T^{-3}$, the root region $\langle\rho(E)\rangle \propto \sqrt{|\varepsilon|}$ near the threshold disappears altogether: the semiclassical number of states becomes smaller than unity in this region. As a result, the subgap density of states, which is determined by the zero-dimensional σ model as before, cannot be described by formula (3.18) any longer, but is given by expression (4.44). This is in agreement with the relation between the root dependence ($\langle\rho(E)\rangle \propto \sqrt{|\varepsilon|}$) of the density of states above the threshold and the applicability of the random matrix theory in zero-dimensional systems, which was noted in [24]. In the limit $\tilde{\gamma} \ll G_T^{-3}$, the tail becomes strong: it contains many energy levels instead of one, as in the case of transparent boundaries. In the intermediate case, $G_T^{-3} \ll \tilde{\gamma} \ll 1$, the asymptotic form (3.18) is realized in the immediate vicinity of the threshold, while the asymptotic form (4.44) is observed for $\tilde{\gamma}^{2/3} \ll \varepsilon \ll 1$; the number of subgap states in this case is on the order of unity.

ACKNOWLEDGMENTS

The authors thank C. Beenakker, D. Ivanov, V. Lebedev, A. Mirlin, Yu. Nazarov, B. Simons, and A. Shitov for numerous fruitful discussions.

This study was supported financially by the Swiss and Dutch science foundations, Russian Foundation for Basic Research (project no. 01-02-17759), the program "Quantum Macrophysics" of the Russian Academy of Sciences, and the Foundation for Assistance to Russian Science (M. A. S.).

APPENDIX A

Parametrization of W Matrix

Matrix W contains eight commuting and eight Grassmann parameters and satisfies Eqs. (2.43). We denote real variables by a, b, c, d, m, n, p, and q. The first four variables parametrize the FF sector, and the last four, the BB sector of W:

$$W^{FF} = \frac{1}{2}(-a\sigma_z\tau_x + b\sigma_z\tau_y - c\sigma_x + d\sigma_y), \qquad \text{(A.1)}$$

$$W^{BB} = \frac{i}{2}\left(m\sigma_z\tau_x + n\sigma_x\tau_z + p\frac{\sigma_y\tau_z - \sigma_z\tau_y}{\sqrt{2}} - q\frac{\sigma_y\tau_z + \sigma_z\tau_y}{\sqrt{2}}\right). \qquad \text{(A.2)}$$

Grassmann variables (λ, μ, ζ, κ, η, γ, ξ, and ω) parametrize the FB sector:

$$W^{FB} = \frac{1}{4}\begin{pmatrix} 0 & \lambda-\mu+\zeta-\kappa & \lambda+\mu+\zeta+\kappa & 0 \\ \lambda-\mu-\zeta+\kappa & 0 & 0 & \lambda+\mu-\zeta-\kappa \\ -\gamma-\eta+\xi+\omega & 0 & 0 & \gamma-\eta+\xi-\omega \\ 0 & -\gamma-\eta-\xi-\omega & \gamma-\eta-\xi+\omega & 0 \end{pmatrix}. \quad \text{(A.3)}$$

The anti-self-conjugate condition $W + \overline{W} = 0$ makes it possible to express the BF sector of W in terms of the FB sector: $W^{BF} = i\tau_x\sigma_x(W^{FB})^T\sigma_y\tau_x$.

We can establish a relation between commuting parameters of W and fluctuations of angles in matrix Q. This relation has the form

$$\begin{aligned} a &= 2\sin\theta_F\delta\varphi_F, \quad b = 2\delta\theta_F, \\ c &= 2\cos\theta_F\delta k_F|_{\chi_F=\pi/2}, \\ d &= 2\cos\theta_F\delta k_F|_{\chi_F=0}, \\ m &= 2i\sin\theta_B\delta\varphi_B, \quad n = 2i\sin k_B\chi_B, \\ p &= i\sqrt{2}\delta\beta, \quad q = i\sqrt{2}\delta\alpha. \end{aligned} \quad \text{(A.4)}$$

It should be noted that variable n at the first instanton corresponds to the zero mode (rotation of angle χ_B).

In order to pass from integration over Q to integration over W, we must calculate the Jacobian of the corresponding transformation. However, this Jacobian is equal to unity, which can easily be established from the following equality:

$$\begin{aligned} \mathrm{str}(dQ)^2 = \mathrm{str}(dW)^2 &= da^2 + db^2 + dc^2 + dd^2 \\ &+ dm^2 + dn^2 + dp^2 + dq^2 + d\lambda d\eta + d\mu d\gamma \\ &+ d\zeta d\xi + d\kappa d\omega. \end{aligned} \quad \text{(A.5)}$$

APPENDIX B

Airy Type Integrals

In this section, we evaluate integral (3.16). Integration with respect to w can be carried out immediately (contour C_1 in Fig. 3). As a result, the density of states will be reduced to the sum of two contributions:

$$\langle\rho\rangle = -\frac{1}{4\pi\Delta_g}\mathrm{Im}[\mathrm{Ai}(\epsilon)\rho_1(\epsilon) + \mathrm{Ai}'(\epsilon)\rho_2(\epsilon)], \quad \text{(B.1)}$$

$$\begin{aligned} \rho_1(\epsilon) &= \int_0^\infty dm \int_{C_3} dl(l^3 + 3\epsilon l - lm + 1) \\ &\times \exp\left(\frac{l^3}{3} + ml - \epsilon l\right), \end{aligned} \quad \text{(B.2)}$$

$$\begin{aligned} \rho_2(\epsilon) &= \int_0^\infty dm \int_{C_3} dl(3l^2 - m + \epsilon) \\ &\times \exp\left(\frac{l^3}{3} + ml - \epsilon l\right). \end{aligned} \quad \text{(B.3)}$$

In order to calculate $\rho_{1,2}(\epsilon)$, we use the following approach. We first eliminate m from the preexponential factor, expressing it in terms of $\partial/\partial l$, then get rid of derivatives by integrating by parts, express l in terms of $\partial/\partial m$, and, finally, integrate with respect to m wherever possible. As a result, the integral with respect to l becomes trivial. Thus, we begin with $\rho_1(\epsilon)$:

$$\begin{aligned} \rho_1(\epsilon) &= \int_0^\infty dm \int_{C_3} dl\left(-l\frac{\partial}{\partial l} + 2l^3 + 2\epsilon l + 1\right) \\ &\times \exp\left(\frac{l^3}{3} + ml - \epsilon l\right) \\ &= \int_0^\infty dm \int_{C_3} dl(2l^3 + 2\epsilon l + 2)\exp\left(\frac{l^3}{3} + ml - \epsilon l\right) \\ &= \int_0^\infty dm \int_{C_3} dl\left(2\frac{\partial^3}{\partial m^3} + 2\epsilon\frac{\partial}{\partial m} + 2\right)\exp\left(\frac{l^3}{3} + ml - \epsilon l\right) \\ &= \left[\left(-2\epsilon - 2\frac{\partial^2}{\partial m^2}\right)\Big|_{m=0} + 2\int_0^\infty dm\right] \\ &\times \int_{C_3} dl\exp\left(\frac{l^3}{3} + ml - \epsilon l\right). \end{aligned} \quad \text{(B.4)}$$

Similarly, for $\rho_2(\epsilon)$, we have

$$\begin{aligned} \rho_2(\epsilon) &= \int_0^\infty dm \int_{C_3} dl\left(4l^2 - \frac{\partial}{\partial l}\right)\exp\left(\frac{l^3}{3} + ml - \epsilon l\right) \\ &= \int_0^\infty dm \int_{C_3} dl\left(-4\frac{\partial^2}{\partial m^2}\right)\exp\left(\frac{l^3}{3} + ml - \epsilon l\right) \\ &= -4\frac{\partial^2}{\partial m^2}\Big|_{m=0}\int_{C_3} dl\exp\left(\frac{l^3}{3} + ml - \epsilon l\right). \end{aligned} \quad \text{(B.5)}$$

The integral with respect to l appearing in the expressions for $\rho_{1,2}$ is given by

$$\int_{C_3} dl \exp\left(\frac{l^3}{3} + ml - \epsilon l\right) = \pi[\mathrm{Bi}(\epsilon - m) - i\mathrm{Ai}(\epsilon - m)]. \quad \text{(B.6)}$$

Substituting $\rho_{1,2}$ into expression (B.1) and using the functional relations for the Airy functions, we arrive at expression (3.18).

REFERENCES

1. *Mesoscopic Phenomena in Solids*, Ed. by B. L. Altshuler, P. A. Lee, and R. A. Webb (Elsevier, Amsterdam, 1991).
2. A. F. Andreev, Zh. Éksp. Teor. Fiz. **49**, 65 (1965) [Sov. Phys. JETP **22**, 47 (1966)].
3. I. O. Kulik and A. N. Omel'yanchuk, Fiz. Nizk. Temp. **3**, 945 (1977) [Sov. J. Low Temp. Phys. **3**, 459 (1977)].
4. J. A. Melsen *et al.*, Europhys. Lett. **35**, 7 (1996); Phys. Scr. **69**, 223 (1997).
5. A. Lodder and Yu. V. Nazarov, Phys. Rev. B **58**, 5783 (1998).
6. D. Taras-Semchuk and A. Altland, Phys. Rev. B **64**, 014512 (2001).
7. G. Eilenberger, Z. Phys. **214**, 195 (1968).
8. A. I. Larkin and Yu. N. Ovchinnikov, Zh. Éksp. Teor. Fiz. **55**, 2262 (1968) [Sov. Phys. JETP **26**, 1200 (1968)].
9. K. Usadel, Phys. Rev. Lett. **25**, 507 (1970).
10. A. A. Golubov and M. Yu. Kupriyanov, Zh. Éksp. Teor. Fiz. **96**, 1420 (1989) [Sov. Phys. JETP **69**, 805 (1989)].
11. F. Zhou *et al.*, J. Low Temp. Phys. **110**, 841 (1998).
12. S. Pilgram, W. Belzig, and C. Bruder, Phys. Rev. B **62**, 12462 (2000).
13. I. M. Lifshits, Usp. Fiz. Nauk **83**, 617 (1964) [Sov. Phys. Usp. **7**, 571 (1965)].
14. L. B. Ioffe and M. V. Feĭgel'man, Zh. Éksp. Teor. Fiz. **89**, 654 (1985) [Sov. Phys. JETP **62**, 376 (1985)].
15. E. Brezin, D. J. Gross, and C. Itzykson, Nucl. Phys. B **235**, 24 (1984).
16. K. B. Efetov and V. G. Marikhin, Phys. Rev. B **40**, 12126 (1989).
17. E. P. Wigner, Ann. Math. **53**, 36 (1951).
18. F. J. Dyson, J. Math. Phys. **3**, 140 (1962); **3**, 157 (1962); **3**, 166 (1962).
19. M. L. Mehta, *Random Matrices* (Academic, New York, 1991).
20. C. W. J. Beenakker, Rev. Mod. Phys. **69**, 731 (1997).
21. K. B. Efetov, Zh. Éksp. Teor. Fiz. **83**, 883 (1982) [Sov. Phys. JETP **56**, 467 (1982)].
22. M. G. Vavilov, P. W. Brower, V. Ambegaokar, and C. W. J. Beenakker, Phys. Rev. Lett. **86**, 874 (2001).
23. A. Lamacraft and B. D. Simons, Phys. Rev. Lett. **85**, 4783 (2000).
24. A. Lamacraft and B. D. Simons, Phys. Rev. B **64**, 014514 (2001).
25. S. F. Edwards and P. W. Anderson, J. Phys. F **5**, 965 (1975); A. Nitzan, K. H. Freed, and M. H. Cohen, Phys. Rev. B **15**, 4476 (1977).
26. K. B. Efetov, *Supersymmetry in Disorder and Chaos* (Cambridge Univ. Press, New York, 1997).
27. A. Altland, B. D. Simons, and D. Taras-Semchuk, Pis'ma Zh. Éksp. Teor. Fiz. **67**, 21 (1997) [JETP Lett. **67**, 22 (1997)]; Adv. Phys. **49**, 321 (2000).
28. A. A. Abrikosov and L. P. Gor'kov, Zh. Éksp. Teor. Fiz. **39**, 1781 (1960) [Sov. Phys. JETP **12**, 1243 (1961)].
29. P. M. Ostrovsky, M. A. Skvortsov, and M. V. Feigel'man, Phys. Rev. Lett. **87**, 027002 (2001).
30. P. M. Ostrovsky, M. A. Skvortsov, and M. V. Feigel'man, Pis'ma Zh. Éksp. Teor. Fiz. **75**, 407 (2002) [JETP Lett. **75**, 336 (2002)].
31. M. A. Skvortsov, V. E. Kravtsov, and M. V. Feĭgel'man, Pis'ma Zh. Éksp. Teor. Fiz. **68**, 84 (1998) [JETP Lett. **68**, 84 (1998)].
32. C. A. Tracy and H. Widom, Commun. Math. Phys. **159**, 151 (1994); **177**, 727 (1996).
33. L. P. Gor'kov and G. M. Éliashberg, Zh. Éksp. Teor. Fiz. **48**, 1407 (1965) [Sov. Phys. JETP **21**, 940 (1965)].
34. T. Guhr, A. Müller-Groeling, and H. A. Weidenmüller, Phys. Rep. **299**, 189 (1998).
35. A. Altland and M. R. Zirnbauer, Phys. Rev. B **55**, 1142 (1997).
36. A. V. Zaĭtsev, Zh. Éksp. Teor. Fiz. **86**, 1742 (1984) [Sov. Phys. JETP **59,** 1015 (1984)].
37. M. Yu. Kupriyanov and V. F. Lukichev, Fiz. Nizk. Temp. **8**, 1045 (1982) [Sov. J. Low Temp. Phys. **8**, 526 (1982)].
38. W. Belzig and Yu. V. Nazarov, Phys. Rev. Lett. **87**, 197006 (2001).
39. B. A. Muzykantskii and D. E. Khmelnitskii, Phys. Rev. B **51**, 5480 (1995).
40. V. I. Fal'ko and K. B. Efetov, Europhys. Lett. **32**, 627 (1995).
41. A. D. Mirlin, Phys. Rev. B **53**, 1186 (1996).
42. B. A. Muzykantskii and D. E. Khmelnitskii, E-print archives, cond-mat/9601045.
43. A. D. Mirlin, Pis'ma Zh. Éksp. Teor. Fiz. **62**, 583 (1995) [JETP Lett. **62**, 603 (1995)].
44. B. L. Altshuler, V. E. Kravtsov, and I. V. Lerner, in *Mesoscopic Phenomena in Solids*, Ed. by B. L. Altshuler, P. A. Lee, and R. A. Webb (Elsevier, Amsterdam, 1991), p. 449.
45. A. D. Mirlin, Phys. Rep. **326**, 259 (2000).

Translated by N. Wadhwa